Materials Innovations

HΣXA Publishers

Quantum Dots | Review Article | http://doi.org/10.54738/MI.2022.21002

Recent Developments in Graphene Quantum Dots in Energy Related Applications: A Review

Ambreen Kalsoom[1]*, Misbah Mirza[2], Zoobia Shah[1], Anam Majeed[1], Shamroza Mubarik[3], Arooj Ali[4], Asma Tariq[1], Tooba Arshad[1], Sawera Ramzan[1], Waseem Akhtar Qureshi[5]

1 Department of Physics, Govt. Sadiq College Women University, 63100, Bahawalpur, Bahawalpur, Pakistan
2 Department of Physics, The Women University Multan, 60000, Multan, Pakistan
3 Department of Chemistry Govt, Sadiq College Women University, 63100, Bahawalpur, Bahawalpur, Pakistan
4 Institute of Physics, The Islamia University of Bahawalpur, 63100, Bahawalpur, Bahawalpur, Pakistan
5 Cholistan Institute of Desert Studies (CIDS), Baghdad-ul-Jadeed Campus, The Islamia University of Bahawalpur, 63100, Bahawalpur, Pakistan

Received: 23 August 2022
Accepted: 10 October 2022
Published: 28 October 2022

Citation: Kalsoom A, Mirza M, Shah Z, Majeed A, Mubarik S, Ali A, Tariq A, Arshad T, Ramzan S, Qureshi WA (**2022**) Recent Developments in Graphene Quantum Dots in Energy Related Applications: A Review. *Materials Innovations 2* (10), 269-297.

***Correspondence**: (Ambreen Kalsoom) kalsoom.ambreen@gscwu.edu.pk

Published By Hexa Publishers

ISSN
Electronic: 2790-1963

Recently, graphene quantum dots (GQDs), zero-dimensional flat nanomaterials with distinct optical, electrical, and optoelectric properties, have attracted significant attention, owing to their non-toxicity and physiological inertness. A variety of top-down and bottom-up methodologies have been exploited for the synthesis of these materials, including electrochemical oxidation, hydrothermal or solvothermal, microwave-assisted, controllable synthesis and carbonization from organic molecules or polymers. This review focuses on the synthesis and applications of GQDs in solar cells, supercapacitors, LEDs, and Li/Na ion batteries. Herein, we summarized in detail the synthesis methods for GQDs employed in energy storage applications with enhanced capacitance, power conversion, retention capability, and stability, achieved by adjusting many synthesis parameters, including annealing temperature, growth time, substrate concentration, and catalyst. The conclusion highlights the potential opportunities and challenges related to future research on GQDs.

Keywords: GQDs, Solar cells, LEDs, Batteries, Supercapacitors, Bottom up, Top down

INTRODUCTION

Graphene is a carbon-based two-dimensional substance which is fabricated of carbon atom layers that form six-member rings[1]. Graphene is the thin and most transparent material, which is the strongest, most flexible crystal, and most impermeable substance[2]. Quantum dots (QDs) are nanoparticles or nanocrystals which are man-made charge ”droplets”. They can hold a single electron or a large number of electrons[3]. Their optical, as well as electrical characteristics are significantly size-dependent[4]. Quantum dots can store information. Across all three spatial dimensions, a quantum dot can limit electron mobility. This produces a collection of finite as well as thin energy levels that resembles what can be seen in atomic physics[5]. Due to their d-function-like

density of states, semiconductor quantum dots are frequently resorted to as artificial atoms. The fact that both free atoms and QDs have optical line spectra with short line width entirely reflects their similarities[6]. So, both Graphene and quantum dots possess different and useful optoelectronic properties due to their nanoscale composition[7]. GQDs are constituted by more than one layer of Graphene sheets with a width of fewer than five nms. GQDs are almost elliptical or disc-like, but quadrilateral and semestral GQDs are also produced[8]. Exciton occupies infinite Bohr diameter in Graphene. As a result, quantum confinement effects will be observed in Graphene fragments of any size. GQDs produced luminescence when stimulated and have some value of bandgap other than zero. This bandgap may be adjusted by changing the GQD's size and surface chemistry. Functional groups on GQDs contribute additional absorption characteristics and impact photoluminescence which is known as the edge effect. Furthermore, based on the synthesis methods and the functional groups, the spectroscopic characteristics of GQDs may be different that is present on the particle's boundaries. The most charming features of GQDs are that they are made up of carbon and therefore readily available, with low toxicity and great solubility in a variety of solvents[9]. Because of the intrinsic inert carbon feature, GQDs are considered a novel type of quantum dot (QD). They are physically as well as chemically stable[10]. Figure 1 indicated the properties of GQDs.

Zero band gap of Graphene is one of its most intriguing characteristics. Pure Graphene has not any band gap; however, that is the key limitation for the variety of Graphene-based applications. Transistors are made-up of zero band-gap Graphene; for example, by providing low on-off ratios despite their quick switching speed. A band gap may be introduced to Graphene quantum structures to modify the material's physical characteristics. GQDs and other quantum-sized variants of Graphene have been created, proceeding toward recent applications in photovoltaic detection, plasmonics and LEDs. GQDs have a unique structure and can be differentiated from graphene due to the quantum confinement effect. When the size of graphene is decreased to the exciton Bohr radius, the quantum confinement phenomenon occurs. The optical and electrical properties of GDQs are influenced by their shape, edge structure, and size. Son et al. predicted one of the first theories on the band structure of graphene[12]. In 2008, Ponomarenko identified the bandgap transitions of GQDs[13]. The □* transition is the cause of the peak around 230–270 nm, while the n □ * transition is responsible for the peak at around 320 nm. The surface state is referred to as the absorption tail. Most of GQDs have emission peaks in the blue to green spectrum area, when being excited by ultraviolet light. In addition, the pH and excitation affect the photoluminescence of GQDs. Under UV light, they show just a little photo-bleaching and are quite stable[14]. The fluorescence property of GQDs allows their fabrication into LEDs. There are two methods to apply them. Firstly, the emitting component can be directly made of luminous elements. And the alternative option is to employ light-emitting materials as just the lighting-emitting chip's color conversion layer. The second one is more reliable because the first method necessitates precise device construction and technological optimization[15]. Figure 2 illustrates the fluorescence applications of GO and GQDs.

GQDs with foreign elements, such as N-doped GQDs and B-doped GQDs, have also been created and studied. Despite all of the enthusiasm surrounding GQDs, their toxicity is a vital element that must be addressed. GQD toxicity is mostly governed by their concentration. The toxicity profile of GQDs differs depending on how they were being synthesized[17].

SYNTHESIS OF GQDs

GQD manufacturing methods are divided into two main categories i.e., top-down and bottom-up strategies[18]. Figure 3 shows how carbon dots are produced using these two strategies.

Top-down strategy

The top-down strategy involves cleaving or downsizing mass carbon compounds. This synthesis approach leads to the production of GQDs with significant surface defects as a result of aromatic framework damage during their size reduction[20]. Furthermore, top-down GQDs often have edge functional groups, making the chemical fabrication of GQDs easier. Nevertheless, these approaches have several drawbacks, including a low yield and impairment of the benzoic carbon framework[21].

Solvothermal and hydrothermal techniques

These approaches produce two-dimensional quantum dots more efficiently. When compared to other methods, it is simple and inexpensive. Water is used as a solvent in the hydrothermal approach, but an organic solvent such as Dimethyl Formamide (DMF) has been used as a solvent in the solvothermal technique[22]. Graphene oxide sheets are unstable and quickly attacked by chemicals to create GQDs. During oxidation, the incoming epoxy functionality is introduced linearly throughout the carbon lattice, and C–C bond breaks down into tiny oxygenated fragments. The reaction generates the cleavage site, allowing graphene oxide sheets to be divided into finer films[23].The process is displayed below in Figure 4.

Pan et al. firstly adopted a hydrothermal method to produce GQDs from GO (Graphene Oxide)

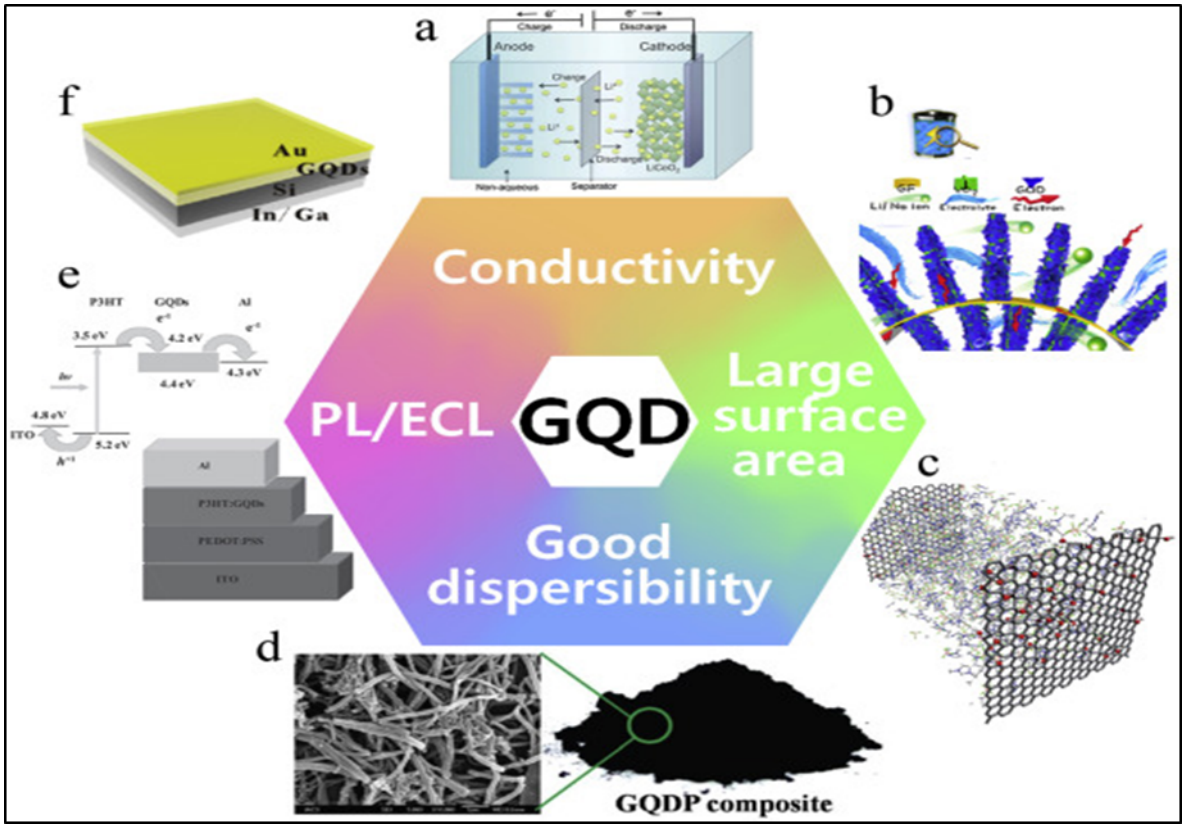

Figure 1. Properties of GQDs. Copyright (2016) Elsevier.[11] *Reprinted with Permission.*

as a starting material. They synthesized GQDs by the oxidation of FO in strong H_2SO_4/HNO_3 acid followed by the initiation of the hydrothermal process under alkaline conditions for around ten hours. Finally, GQDs having 5–13 nm of size distribution were manufactured[24]. It is, however, risky due to the elevated pressure and temperature, and it is time-consuming, taking at least five hours[25]. In 2013, Liu et al. created N-doped GQDs with a diameter of about 2.5 nms. DMF was employed as a solvent, while graphene oxide (GO) was used as a precursor. DMF decomposed at 200°C to generate dimethylamine, which was then used to nitrate graphene oxide for 4–5 hours at 200°C[26]. Figure 5 illustrates the solvothermal approach by which we can synthesize GQDs.

Electrochemical oxidation

At a high redox voltage, C-C bonds in graphene are oxidized and degraded into GQDs. Hydroxyl and oxygen radicals can help in the complexation of electrolytic unpaired electrons (e.g., BF_4^-, $S_2O_8^{2-}$). Li et al. created Jade-luminescent functional GQDs with a consistent diameter of 3–5 nm via redox reactions of a graphene electrode in the solution of phosphate buffer as shown in Figure 6. The oxidation process of a graphene electrode in phosphate-buffered saline yielded 50 GQDs. The groups containing oxygen on the GQDs' plane offered aqueous solubility and made additional research possible. Functionalization of the surface GQDs created by electrochemical oxidation had topographic heights of 1–2 nm and was made up of 1–3 Graphene layers. Hydroxyl and oxygen radicals have a significant inter-graphene attraction to the graphite edge planes, facilitating the intercalation of the BF_4 anion[28].

Zhong and Swager demonstrate that Graphite is activated by propylene carbonate solutions carrying lithium perchlorate, in which graphite foil is immersed. Individual graphene sheets can be functionalized leading to higher graphite expansion. Propylene carbonate is co-intercalated with lithium ions and because of this; the foil of graphite is extended during this preconditioning process. Due to the electrode composition of the intercalated TBAs, positive charges are neutralized. The electrolyte solution is treated with a solid-electrolyte-interphase (SEI) layer, and the applied potential is kept constant at 0.5 V for 24 hours. Extensive washing can eliminate the SEI layer, as evidenced by the drastically diminished XPS O1s peak. Lastly, they demonstrated that the electrochemical functionalization of this hyper-

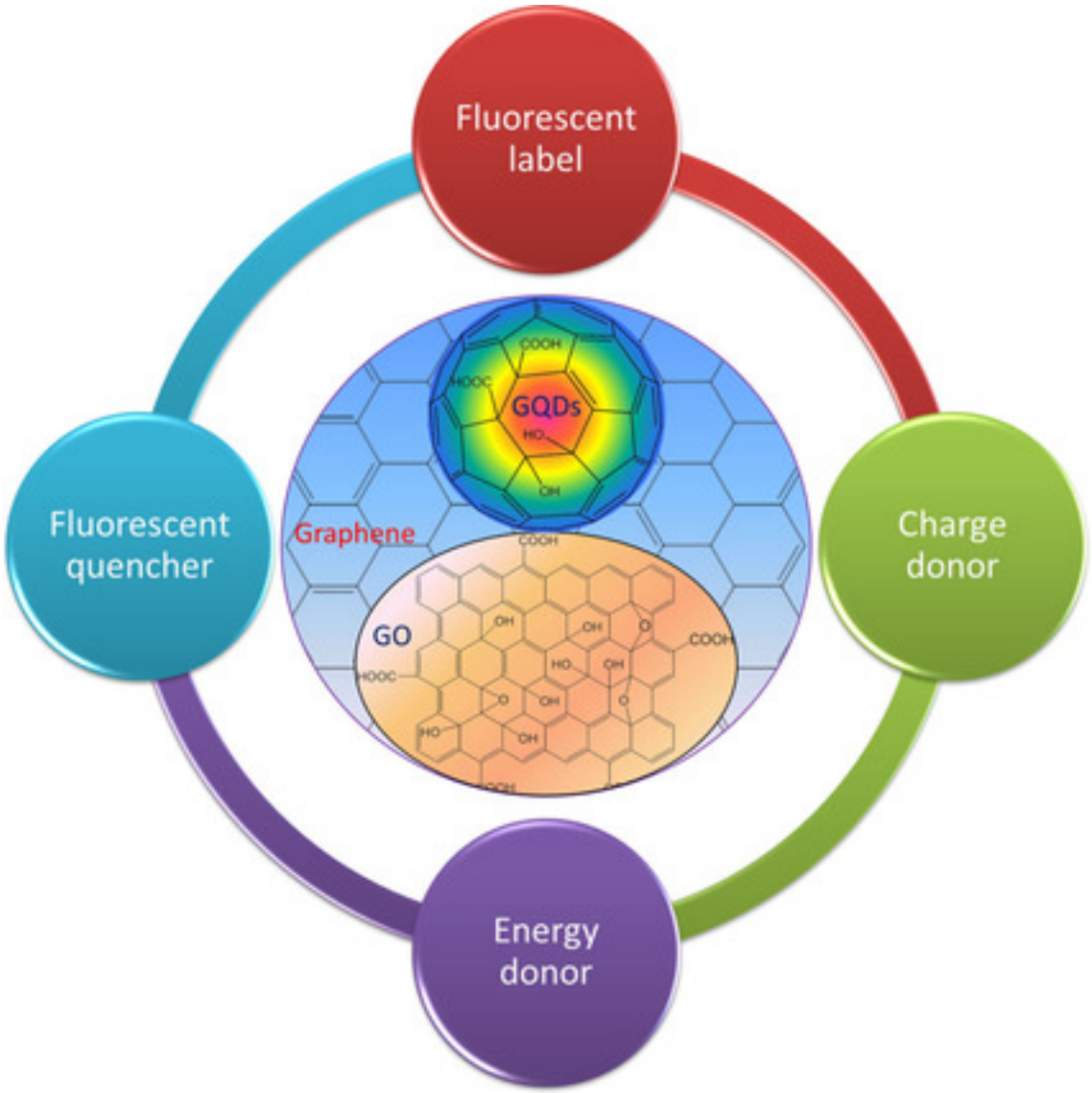

Figure 2. Fluorescence and Sensing Applications of Graphene Oxide and Graphene Quantum Dot. Copyright (2017) Wiley Online Library.[16] *Reprinted with Permission.*

expanded EEG with diazonium salts has improved. Due to electrochemically produced SEI layers inside the lattice of graphite, they worked as stable spacers. This enables a way to synthesize novel graphene and nanocomposite materials[30].

Microwave-assisted techniques

The microwave method makes use of the heat produced by microwave energy produced by three-dimensional polar solvent molecular rotation with an electrical dipolar. This microwave-assisted approach can be used to make high-yield organic and inorganic compounds in a short period. Luo et.al, have published a two-stage microwave-assisted hydrothermal approach for producing white-light-radiating GQDs (WGQDs)[31]. The WGQDS are produced by heating GQDs for 8 hours at 200°C through microwave-assisted extraction and irradiation[32]. Li et al. processed graphene oxide nanosheets in acid for three hours under microwave radiation to produce green-yellow fluorescent GQDs. GQDs with transverse lengths of 2–7 nm and thicknesses of 0.5–2 nm was obtained. The GQDs' luminosity shifted to brilliant blue after further decrease with $NaBH_4$, whereas, their shape and size did not change[33]. Zhang et al. reported the production of GQDs utilizing the microwave-assisted pyrolysis method. In a beaker filled with 20 ml of deionized water, aspartic acid ($C_4H_7NO_4$) along with NH_4HCO_3 were added and heated for 10 minutes

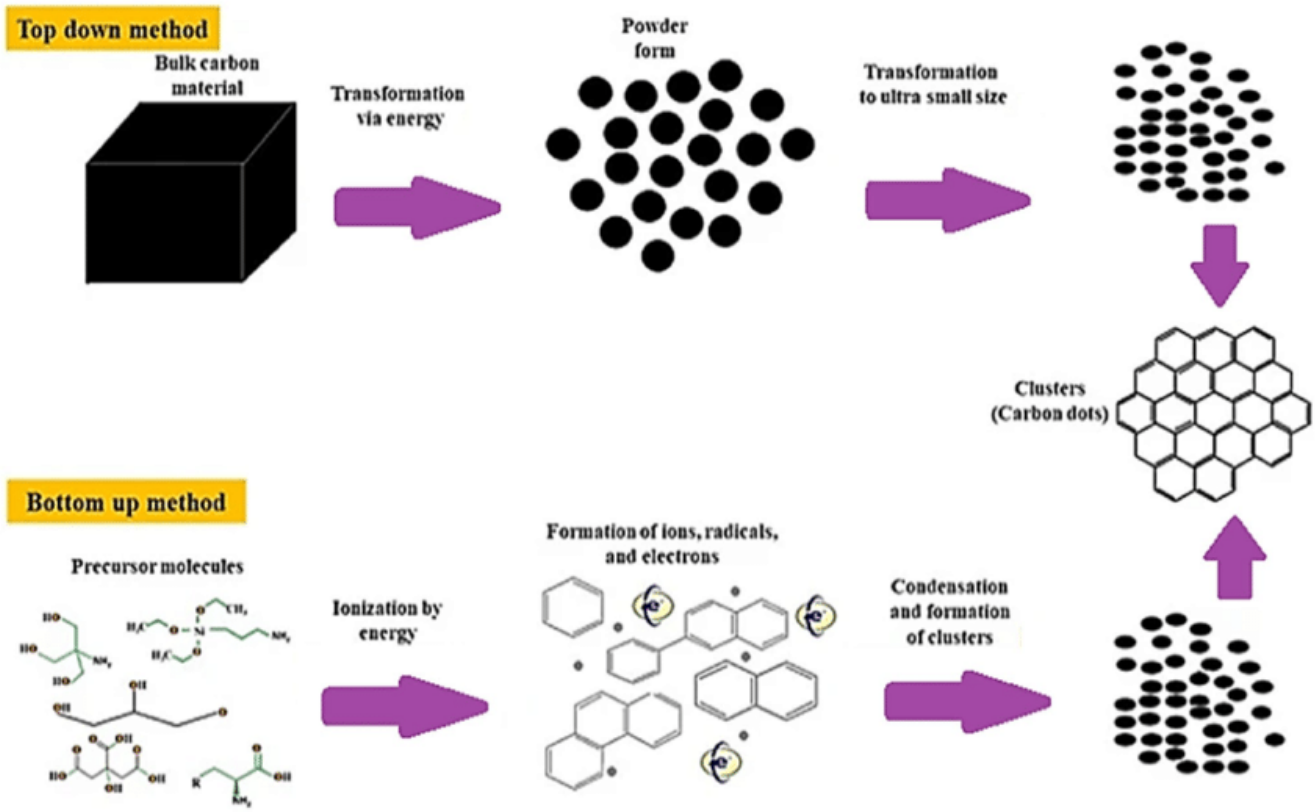

Figure 3. Carbon dots produced using top-down and bottom-up approaches. Copyright (2020) Springer.[19] *Reprinted with Permission.*

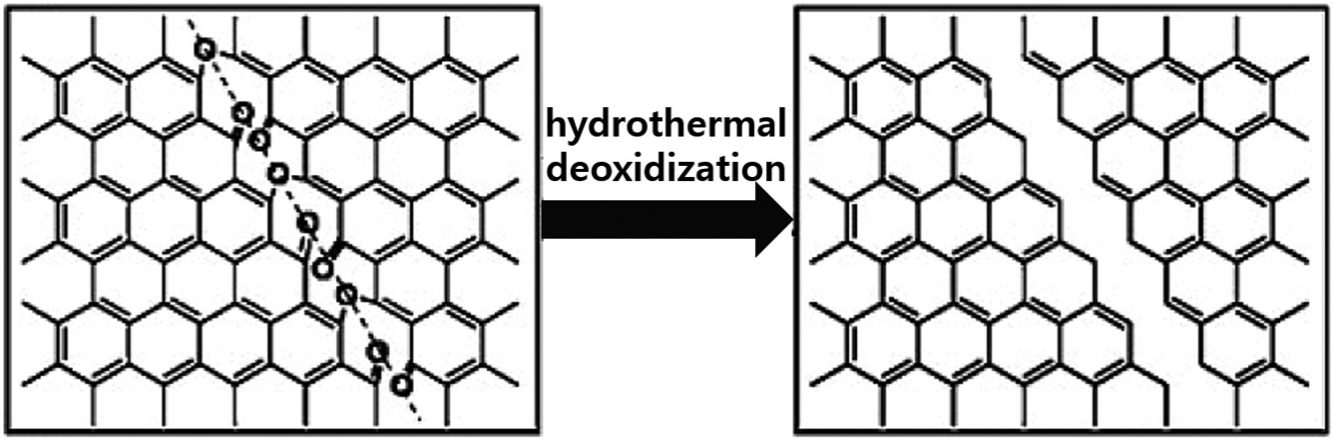

Figure 4. Schematic diagram representing the mechanism of conversion of oxygen-enriched GSs into GQDs via hydrothermal treatment. Copyright (2012) Royal Society of Chemistry.[7] *Reprinted with Permission.*

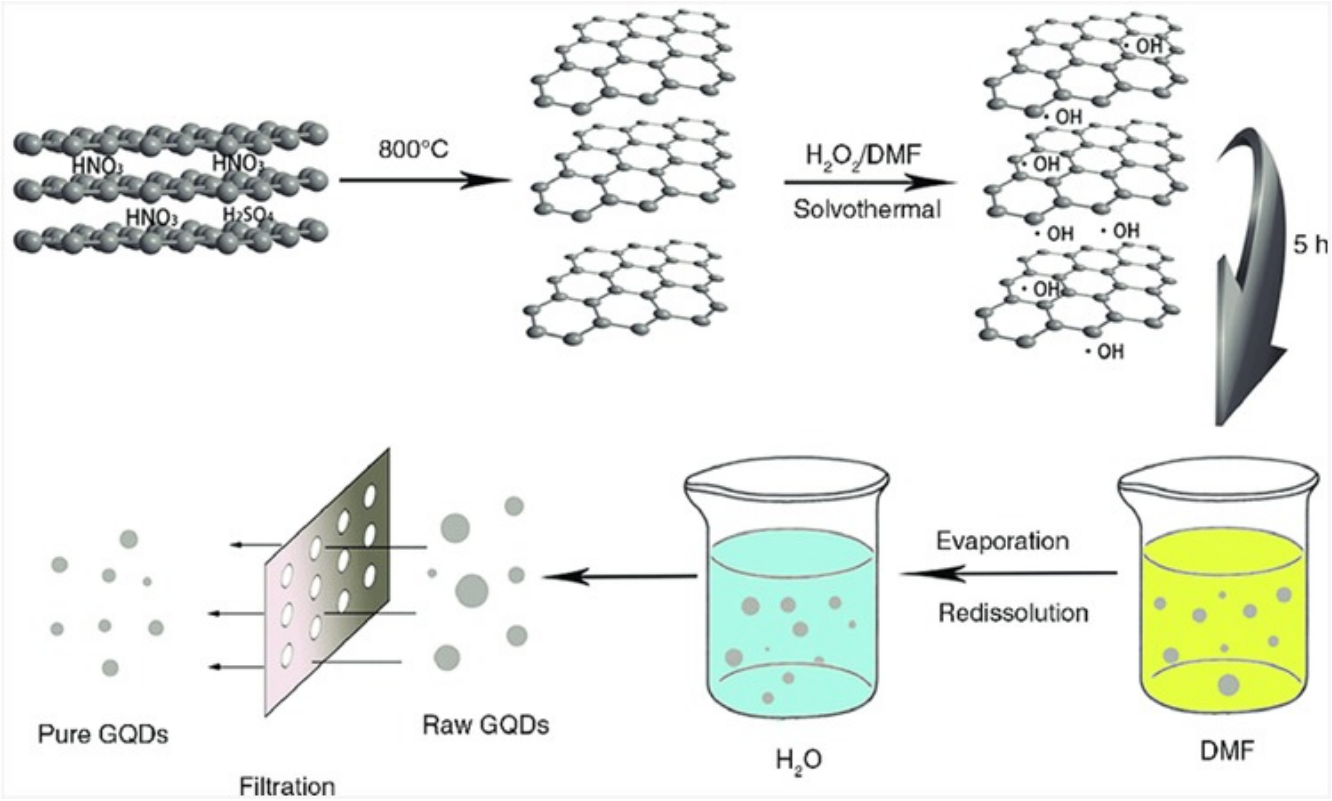

Figure 5. Schematic representation of GQDs prepared by solvothermal method. Copyright (2016) Elsevier.[27] *Reprinted with Permission.*

using microwave irradiation. To get the final GQD, the materials have been further filtered for seven hours. GQD diameters are mostly found in a small range of 1.8–2.4 nm, having an average size of about 2.1 nm[24]. The process for making GQDs is schematically illustrated in Figure 7. After being subjected to pyrolysis, waste is turned into carbon-rich biochar, which is subsequently microwave-treated to provide high yields of GQDs.

Bottom-up strategy

The bottom-up technique depends upon the assembly of microscopic cyclic constituents, either natural or synthetic (e.g., hexaperi-hexabenzocoronene, polyphenyls) with desirable size, morphology, and proportion to control the parameters of the size of the corresponding GQDs. The bottom-up methods are characterized by lengthy procedures[34]. The microwave technique, controllable synthesis[22], molecular carbonization and electron beam irradiation (EBI) procedures are some of the bottom-up approaches[10,32,35]. Figure 8 shows a schematic explanation of a bottom-up method for producing GQDs.

Microwave technique

Since the prolonged rate of reaction of the hydrothermal approach can be considered as a genuine problem, microwave technology has advanced into an instant heat up source that is commonly used during fabrication of nanoparticles. It has not only shortened reaction time however also enhanced productivity[37,38]. Tang et al., were the first to observe intense ultraviolet emission by GQDs at 303 nm while stimulated by a 197 nm laser. That is considered as lowest emitting wavelength observed from organic or inorganic QDs in solution. The size of glucose-derived nanostructures does not affect their emission wavelength, which is being regulated starting from 1.65 to 21 nm by increasing the heating period from 1 to 9 minutes[39]. To purify GQDs, Zhang et al., used NH_4HCO_3 and aspartic acid $C_4H_7NO_4$ as raw resources, deionized water, and microwave-treated GQDs for ten minutes, as well as a filtration membrane for seven hours. The GQDs created emitted an intense blue luminescence, and had a quantum yield of 14%. The significant photoluminescence quenching impact of Fe^{3+} GQDs could be used to detect general metal ions in a very careful manner[40]. The microwave technique significantly decreases the amount of time required to synthesize GQDs, which can now be achieved in moments and treated with a range of influences, expanding the kinds and functionalities of GQDs[25].

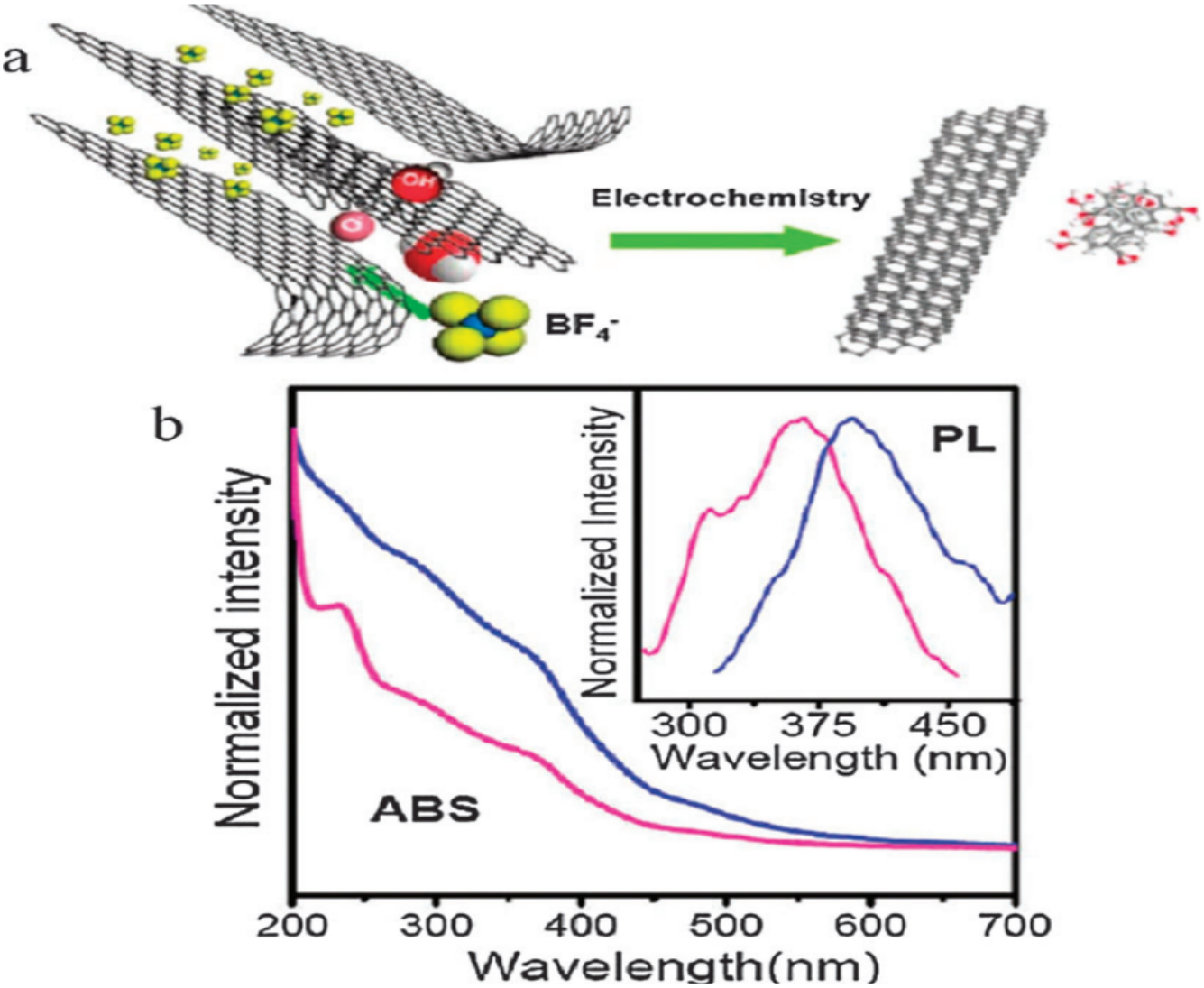

Figure 6. (a) Illustration of the exfoliation process showing the attack of the graphite edge planes by hydroxyl and oxygen radicals, which facilitate the intercalation of BF_4 anion. The dissolution of hydroxylated carbon nanoparticles gives rise to fluorescent carbon nanoparticles. Oxidative cleavage of the expanded graphite produces graphene nanoribbons. (b) UV-vis absorption and fluorescence spectra obtained for 8–10 nm carbon nanoparticles (red curve) and carbon nanoribbons (blue curve). The emission spectrum was obtained using 260 nm excitation. Copyright (2009) American Chemical Society.[29] Reprinted with Permission.

Controllable synthesis

Using this method, GQDs are manufactured from phenyl-containing substances by means of a sequential synthesis method in an organic solvent. The synthesized GQDs have an exact number of carbons and are homogeneous in shape and size. The method of preparation, on the other hand, consists of multistep complex chemical reactions that not just take a substantial amount of time but also provide a low production[25]. Li et al. used this approach to create GQDs of 168, 132, and 170 atoms of carbon indicated by 1, 2, and 3 as illustrated in Figure 9A. TPM molecules (2′, 4′, 6′-trialkyl phenyl) were added to GQDs' borders to avoid them from reuniting. The steric electronic barrier generated by TPM stretching in three dimensions reduced the possibility of GQDs overlapping with one another and increased the phase of dispersion in the organic layer. The graphic depicts the synthesis of 1–3. It begins with tiny molecules like 3-to-4-bromoaniline (representing by 4) and some other modified benzene derivatives to produce two vital precursors, 5 and 6, respectively. Then 1–3 produce polyphenylene dendritic progenitors, which are then used to prepare GQDs by getting

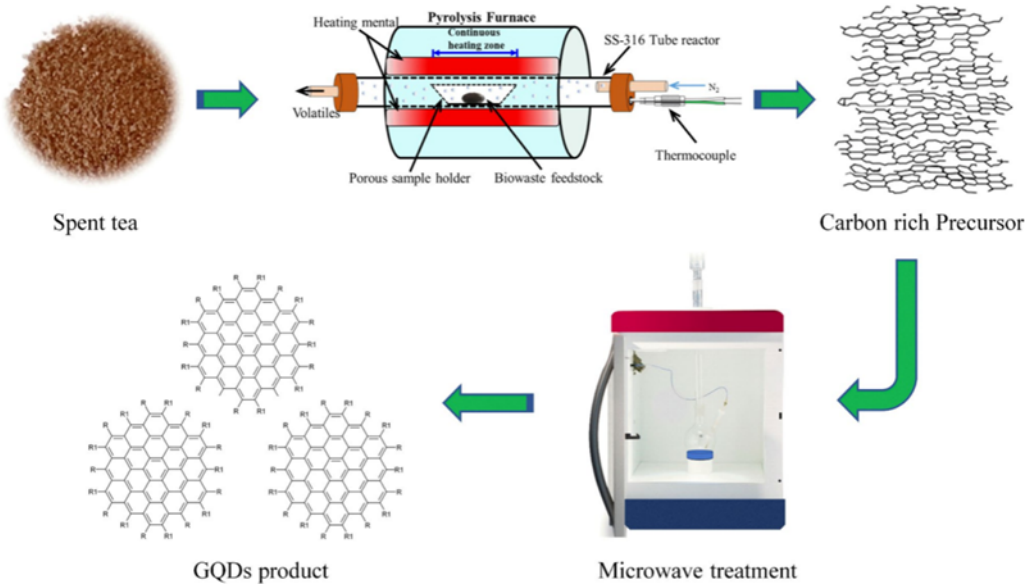

Figure 7. A schematic illustration of the synthesis procedure for GQDs waste is subjected to pyrolysis treatment and carbon rich biochar is obtained, which is then microwave treated to produce GQDs with high yield[23]. Reprinted with Permission.

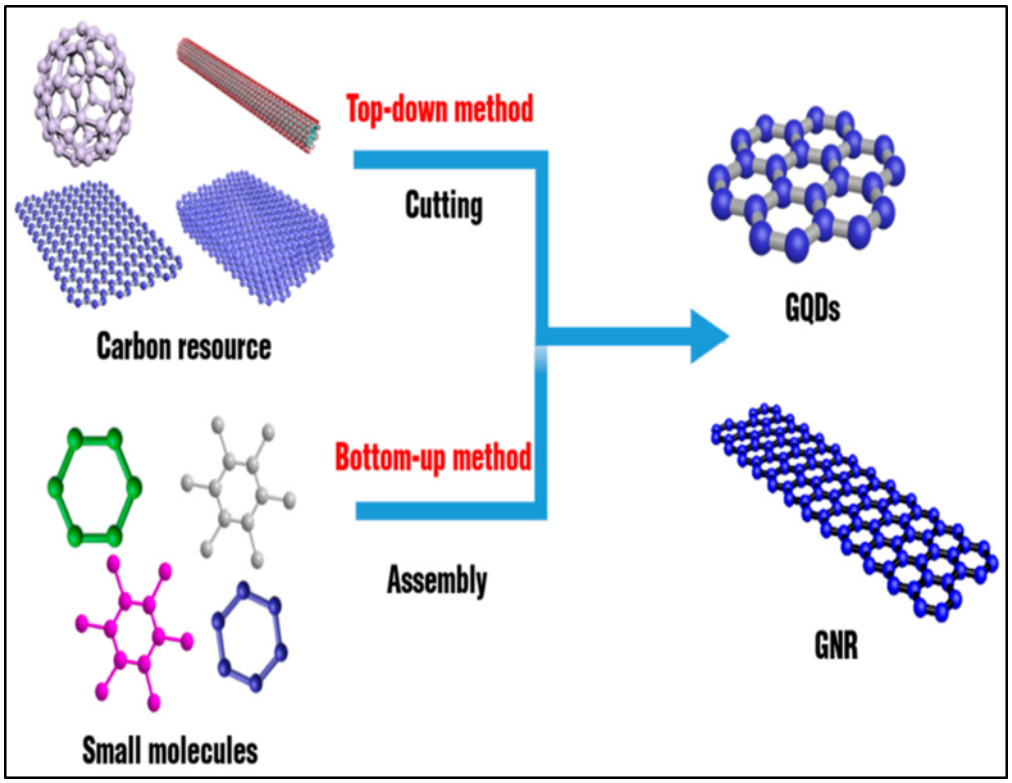

Figure 8. Schematic diagram of top down and bottom up methods for synthesizing GQDs and GNRs.[36] Reprinted with Permission.

treated with an abundance of $FeCl_3$ in a dichloromethane/nitromethane mixture[41]. Wang et al., have established a bottom-up technique for producing GQDs with excellent crystallization and high yield utilizing pyrene as the antecedent. Moreover, the pyrene-derived GQDs developed primarily, include -OH groups, which are difficult to functionalize with biomolecules[42].Chen et al., also created pyrene-derived GQDs with -COOH groups that emit green PL without needing to be excited. GQDs had consistent sizes, a higher PL quantum yield (QY), and were simple to functionalize. GQDs being coupled with monosaccharide for the first time to allow for targeted imaging of carbohydrate receptors on cell membranes, merged in the graphene lattice[43].

The molecular carbonization method is a straightforward and eco-friendly technology that utilizes appropriate polymers or organic molecules for further carbonization and dehydration[44–46]. In the traditional synthesis, glucose granules were soaked in distilled water for 8 hours. The initial sample was translucent (colorless), but as single-layer GQDs (SLGQDs) were created, it turned orange. During the hydrothermal treatment, sugars are dried, resulting in C=C, the primary principle of the graphene. During QD production, one glucose molecule's hydrogen atoms interact with the hydroxyl groups of another, resulting in the synthesis of water molecules. When the sample's peaks do not shift with various emission wavelengths and the emission peak wavelength stays about 540 nm, the result is green photo luminescent[22]. In a standard GQD preparation process, 2 gram of citric acid (CA) was placed in a beaker of size 5 ml along with heated up to 200°C with the help of heating mantle in a conventional GQD preparation technique. The CA got liquefied in around 5 minutes. In 30 minutes, the liquid's color turns from clear to pale yellow and then orange. The orange fluid would eventually convert to black solid in approximately 2 hours if the heating was kept on, indicating the creation of GO. The generated GQDs have a width of 15 nm and a diameter of 0.5–2.0 nm. They exhibit high (9.0%) PL quantum yield as well as excitation-independent PL emission activity. On the other side, GO nanoparticles, typically made up of layers with a width of hundred nm and an altitude of less than one nm[22]. Further, Teymourinia et al., generated GQDs with the use of maize flour as a green forerunner as shown in Figure 10. GQDs of diameters of 20–30 nm were fabricated. At the excitation wavelength of 360 nm, photoluminescence showed broad emission centered at 450 nm. A large peak at 365 nm was observed in the photoluminescence excitation spectra (PLE)[47]. Since the basic structure is difficult to control accurately in this technique, GQDs with polydispersity are created. This method was utilized to generate high-yield and low cost green-photo luminescent GQDs using only distilled water and glucose as a forerunners[48].

By varying the carbonization extent of citric acid and distributing the carbonized derivatives into alkaline solutions, as shown in Figure 11, an ordinary carbonization approach for the production of both GQDs and graphene oxides has been created[44]. Furthermore, Naik et al., described the pyrolysis of citric acid as well as the fabrication of sodium hydroxide to maintain the pH for GQD manufacture. The hydronium ion produced by the CA decomposition functions as a stimulant in the subsequent reduction process. Aromatization and aromatic cluster establishment are accomplished by using aldol condensation and cycloaddition, followed by the introduction of sodium hydroxide. At a various pH, GQDs are finally formed. In this study, the pH was important factor for the manufacturing of GQDs from CA[35]

Electron beam irradiation (EBI) process

It is noteworthy that the electron beam irradiation approach necessitates costly specialized tools and raises the chances of exposure to radiation, thus it isn't widely used[49]. Wang et al., used electron beam irradiation to create monoluminous GQDs at room temperature. A solution of hydrazine hydrate was taken to dissolve 1, 3, 6-trinitropyrene. After stirring, the product was placed in plastic container and was bombarded in a dynamitron electron accelerator through a titanium window as shown in Figure 12. Following ionizing radiation, the specimen was dialyzed for two days with a 0.22 millimeter highly porous membrane filter and a filtration bag, giving GQDs with a QY of 32%. Under the same conditions, small molecules such as urea, 1-Nitropyrene, and citric acid can also be processed as substrates to generate GQDs[42].

However, the bottom-up techniques have time-consuming and difficult synthesis procedures, as well as low production[34]. Thus, the top-down process is frequently used in the production of GQDs in general[22].

APPLICATIONS OF GQDs IN ENERGY STORAGE DEVICES

Solar cells

GQDs are playing a major role in advancements in energy-related applications. Photovoltaic cells are one of the greatest energy-related applications. So, GQDs are modified to improve their efficiency and working capabilities. Applications of GQDs diverge with the types of solar cells. Among various types, there are different ways to insert and use GQDs to enhance their performance. Let it be perovskite photovoltaic cells, dye-sensitized photovoltaic cells, heterojunction photovoltaic cells, organic or any other type, GQDs, and their doped forms are promising in improvising quality of these solar cells. Wang, Z.,

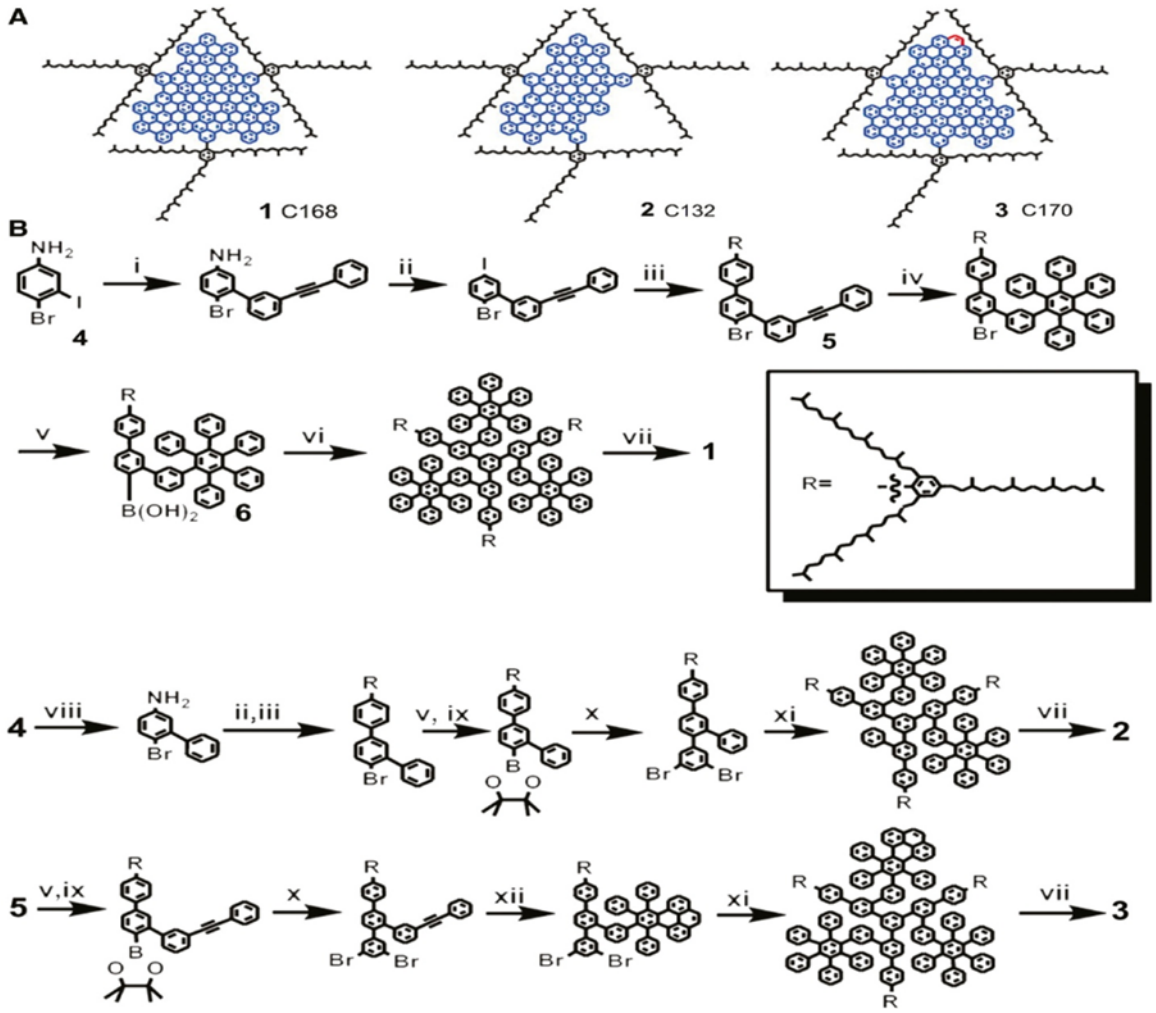

Figure 9. The synthesis process of GQDs and their molecular structures (A) Structure of GQDs 1–3. (B) Synthesis of GQDs 1–3. Copyright (2010) American Chemical Society.[41] *Reprinted with Permission.*

et al. considered the role of GQDs in reversed flexible perovskite photovoltaic cells. In the NiO_x film, GQDs with the amino-functional group were used as a dual-role supplement. They provided an abundance of nitrogen atoms on the improvised nitric oxide layer. Flexible PSCs based on A-NiO_x increased band structure in between hole transport layer (HTL) and perovskite monolayer. The device's photovoltaic performance improved as the number of amino-functionalized GQDs (AGQDs) increased. Figure 13 depicts the effect of AGQDs being fabricated in NiO_x film of perovskite photovoltaic cell[50].

Bian, H., et al. examined Inorganic γ-$CsPbI_3$ Perovskite Photovoltaic Cells, in which Nitrogen-doped GQDs (N-GQDs) change dangerous ultraviolet luminance into beneficial visible photons, resulting in increased solar cell effectiveness. It harvests light in a short wavelength range by acting as energy-down-shift (EDS) film on top of the γ-$CsPbI_3$ PSCs. The optimized PSC has a higher short circuit current density (J_{SC}) of 19.15 Am/cm^2 and a PCE of 16.02%. The doping concentration of N-GQDs is 5.2 %, implying that N has been readily integrated into the GQDs. If the N-GQDs EDS layer is excessively rigid, this can scatter significantly more photons than the flat plane. As the amount of N-GQDs EDS layers increases to 2, the PSCs' J_{SC} grows considerably. As a result, the PCE and J_{SC} are enhanced leading to better device performance[51]. In Figure 13(a), under illumination, a diagram of the transfer of hot electrons to SnO_2 from GQDs is shown. 13(b) shows work function fluctuation of SnO_2 and SnO_2, 13(c) depicts SnO_2 mobility as well as electron trap and 13(d) highlights the space-charge-limited current (SCLC) method is useful to determine SnO_2: GQDs. The maximum steady-state efficiency of planar PSCs based on SnO_2: GQDs ETLs is 20.23 %. In terms of average PCE (19.21.0 %) and J_{SC}, the devices outperformed the bare

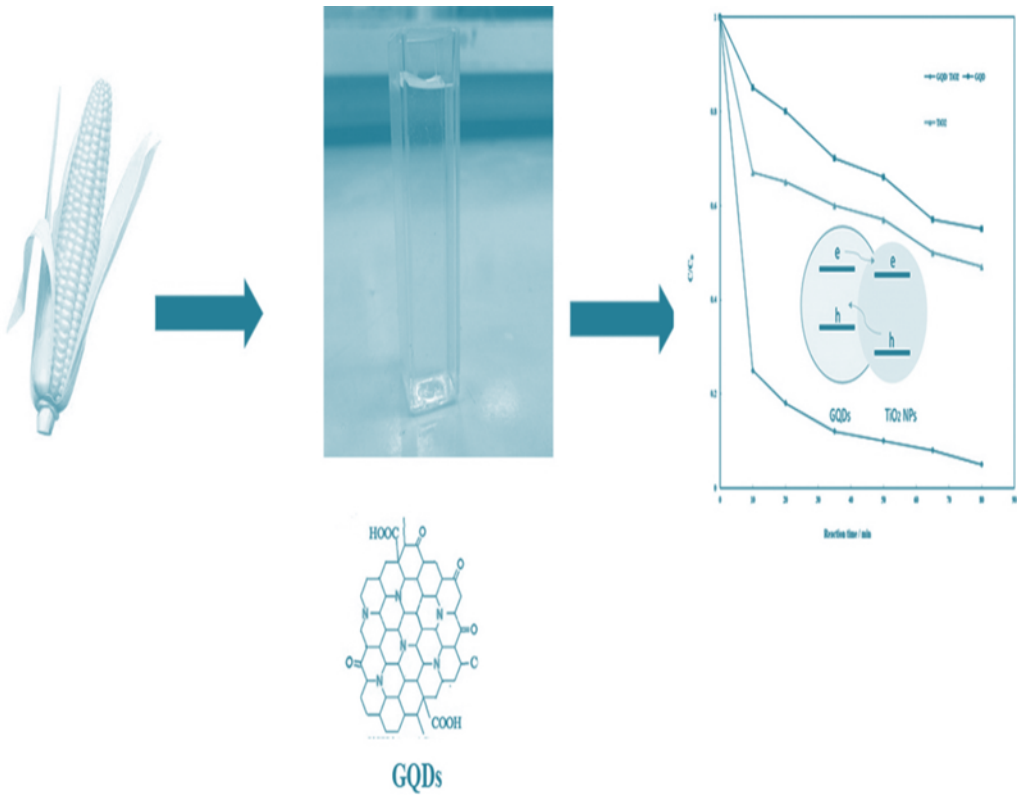

Figure 10. The Corn flour being used to synthesize GQDs. Copyright (2017) Elsevier.[47] *Reprinted with Permission.*

SnO_2 (22.60.9 %)[52].

Using properties of GQDs, J. Zhang et al. were successful in improving the efficiency of planar perovskites. GQDs were synthesized and incorporated into a perovskite substrate. In the crystallization of PF (perovskite film), the incorporation of GQDs is critical. PSCs containing 0.1 % GQD have an 11 % increase in PCE when compared to pristine PSCs[53]. Gao, Z.W., et al. applied Imidazole-Graphene-Quantum-Dots to control the interface in $FAPbI_3$ plane perovskites. Bromide imidazole I-GQDs (functionalized GQDs) control the interface linking the perovskite layer of Formamidinium Lead Iodide ($FAPbI_3$) along with the electron transport layer (ETL). The use of GQDs may enhance ETL conductivity and energy level alignment, resulting in better interface carrier transfer. In addition, the functional groups on top of I-GQDs benefit from the production of high-quality perovskite films, which minimize non-radioactive recombination inside the perovskite film and improve PSC stability without affecting the bandgap of the FA-based perovskite layer[54]. D.S. Ahmed et al. investigated the effect of GQD integrated with a planar ZnO on the effectiveness of a solar cell based on $MAPI_3$ PVK. Planar ZnO: GQD is an economical and eco-friendly additive used to create a hybrid photo electrode in the PSCs of $MAPI_3$ PVK-based solar cells. The results show that 2% of GQD can enhance the PVK surface characteristics, containing surface structure, as well as suppress residual PbI_2 and reduce grain boundaries. After 1500 hours of storage at 60 % and 80°C RH, the foremost stable PSC retained 80 and 90 % of its original efficiency. Furthermore, the ZnO: GQD ETL in the cell design enhances electron accumulation and transport at the ETL/PVK intersection, which enhances the incident photon to current efficiency (IPCE) and Jsc due to the phenomenon of luminescence-quenching[55]. Shin, D.H., et al. Reported that when the concentration of GQDs is increased by the amount of 2.5 mg/L, there noticed to be an increase in the PCE of the PSCs with the grapheme/3-aminopropyl triethoxysilane (GR/APTES) up to 16.4 and there was a 15% increase in flexibility and stiffness substrate respectively. Flexible PV cells also contain 80% of their starting PCE after 3000 curving cycles having a 4 mm curvature. The enhanced flexibility of the APTES junction resulted in excellent bending stability, with flexible PSCs retaining 80% of their beginning PCE after 3000 bending cycles of 4 mm radius[56]. To achieve superior photovoltaic performance, the electron transport layer determines the property of charge transport. To make perovskite solar cells of high efficiency, a simple process for incorporating tiny GQDs on the plane of mesoporous TiO_2 has

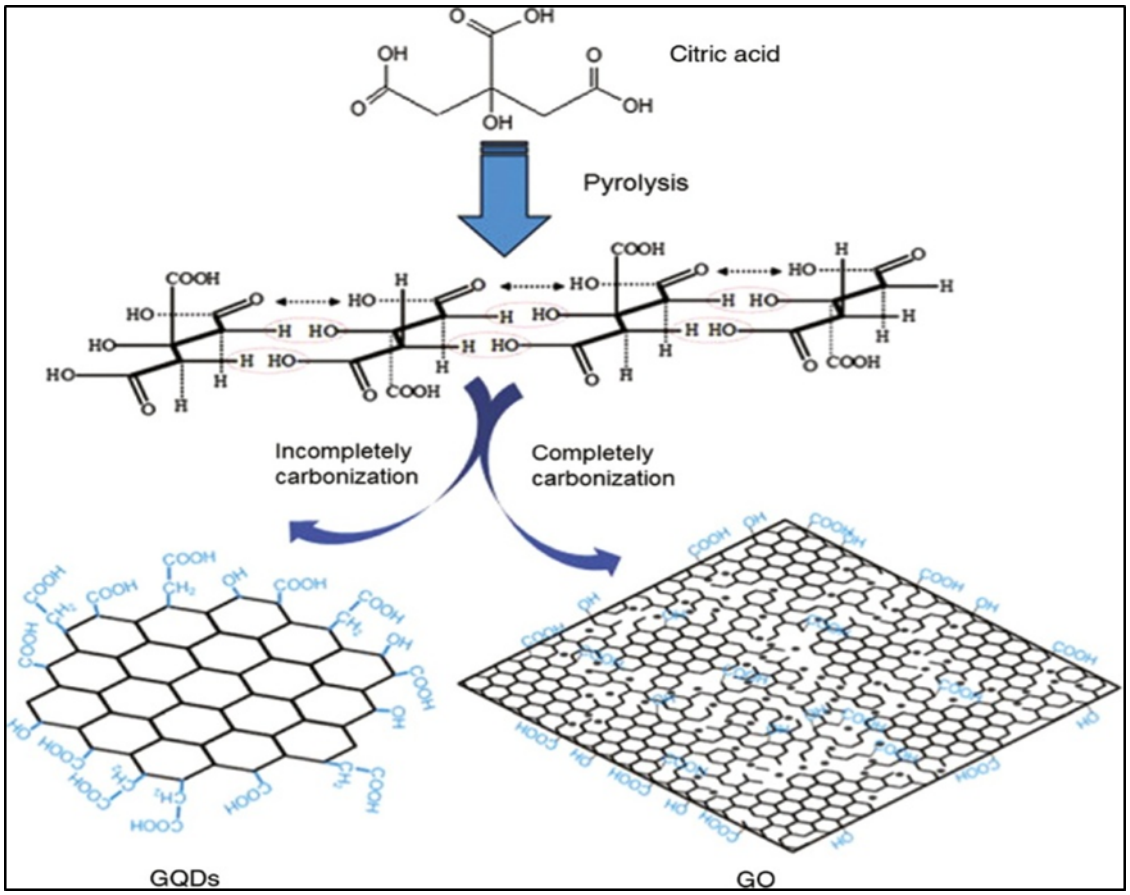

Figure 11. Diagram for the synthesis of GQDs and GO. The black dots in the GO represent oxygen atoms. Copyright (2012) Elsevier.[44] Reprinted with Permission.

been used by Shen, D., et al. The maximum steady-state efficiency of the GQD/mp-TiO_2-based PSC as the layer of electron-transporting was 20.45 %. This efficiency is slightly greater than the efficiency of 18.57 % attained without the pattern[57].

Dye-sensitized solar cells (DSSCs) also showcased enhanced performance by the fabrication of GQDs in them. An experiment was made by Kumar, M.P., et al. to elaborate those Boron-doped GQDs functioned as effective photo anodes for DSSCs and the results demonstrated higher power conversion efficiency[58].

Dinari M. et al. reported that the PANI–GQD nanocomposites electrode-based DSSC's efficiency of energy conversion are observed to be 1.6 %. The dye molecules' panchromatic light absorption, excellent electrolyte ion transport, and efficient redox electrolyte reduction are all important factors for highly productive DSSCs. This is because the electrode has a higher electrochemical activity than the PANI electrode. Fig 14 illustrates the graphs obtained between potential and current density and wavelength and IPCE[59]. In a photo electrode, quantum dots enhance dye and light penetration. Multiple exciton generation ((MEG) is a phenomenon observed in some quantum dots. Quantum dots have the potential to minimize the use of dye in DSSCs while improving performance. At TiO_2 films, GQDs exhibited a strong absorption spectrum as well as photoluminescence (PL) emission[60]. Nm-sized GQDs having a greater amount of defect sites at the edges exhibit exceptional electro-catalytic processes in the hybrid counter electrode (CE) for the reduction of I_3. Fast electron channels for charge inoculation between the GQD and the DSSC substrate are provided by the finest GFs with enhanced electronic conductivity. Chang, Q., et al. achieved efficiencies of up to 9.59 % which is greater than the other Dye-Sensitized Solar Cells that use Pt as the CE (8.58 %). This recommended that small-size GQFDs with more active defects may behave similarly to a Pt electrode[61]. According to Fang, X., et al., the DSSC with the most GQDs performed best, with the lowest dye-adsorption and the largest Jsc of 14.1 $\pm$ 0.02 $mAcm^{-2}$ and 6.10 $\pm$ 0.01 %, respectively. Reduced dye use is critical for the DSSCS's low-cost and environmental friendly design[62].

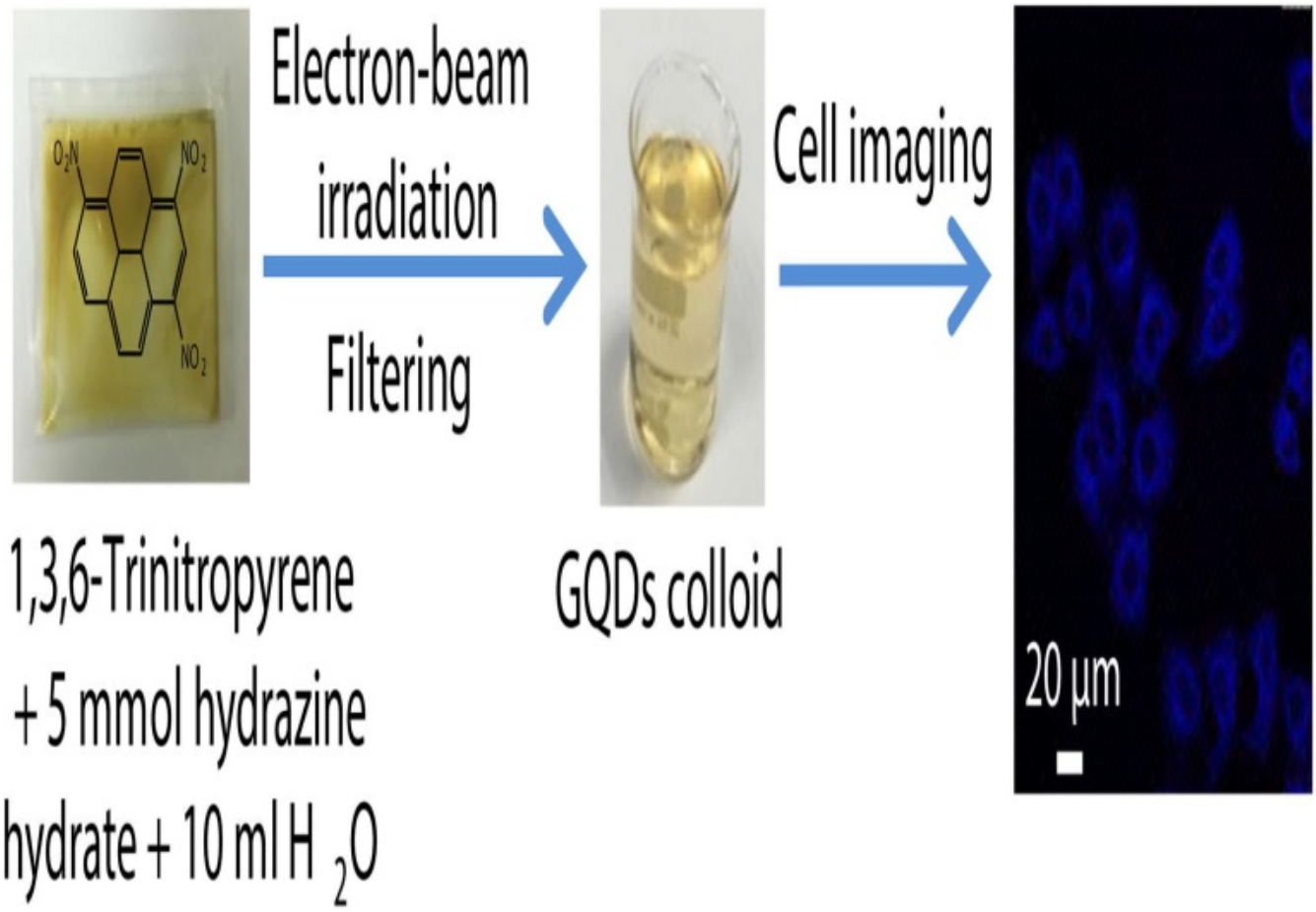

Figure 12. Formation of GQDs through the process of EBI. Copyright (2017) Elsevier.[42] *Reprinted with Permission.*

G. Zamiri and S. Bagheri studied the dye-sensitized solar cell's functionalization using ZnO nanoparticles of varying thicknesses as a photo electrode. The current-voltage (I-V) tests show, that enhancing the diameter of photo-anodes improves the DSSC's efficiency. The photo-generated electrons must travel a longer path to get to the active electrode as the thickness escalates, increasing the wage of electron rejoining. The efficiency increased when they replaced N-719 with GQDs[63].

Looking up at hetero junction's solar cells, Tsai, M.-L., et al. was able to enhance the efficiency of silicon-heterojunction (SHJ) photovoltaic cells, which is represented in Figure 15, through photon's organization by applying as down conversing. The GQD effect allows for more photons to be absorbed in the depletion region, resulting in a stronger photovoltaic effect[64]. An innovative type of solar cell was created by Gao, P., et al. using the c-Si Graphene Quantum Dot's heterojunction. At the junction interface, it was possible to successfully split the photo-generated electron-hole pairs. By changing the size and diameter of the layer, an optimal PCE of 6.6% was achieved[65]. GQDs play a crucial function in charge carrier separation and improving visual absorption rate. A resonance effect is caused by the existence of functional groups having non-bonding electrons, which helps secondary activation at 328 nm[66].

GQDs can be used in organic photovoltaic (OPV) cells as hole transport layers (HTLs). GQDs of the same sizes and high conductivity are superior Hole Transport Layers in PSCs and small molecule solar cells (SMSCs). Li, M., et al. found that PCEs of 3.52, 2.77, and 3.51 % in cells containing PEDOT: PSS, GO, and GCDDs (1.5–2 nm). GQDs were used as HTLs in both PSCs and SMSCs to create high-performance OPV cells[67]. The Efficiency of luminescent solar concentrators was improved by Saeidi, S., et al. with the use of up-converted N-GQDs. Up conversion photoluminescence (UCPL), which emits monochromatic photons in the UV–Vis-NIR range, has already been established. Nitrogen doped GQDs (NGQDs) exhibit up conversion emission, allowing for the use of the NIR region, which is responsible for 52 % of the solar spectrum. Excitation independent of normal PL

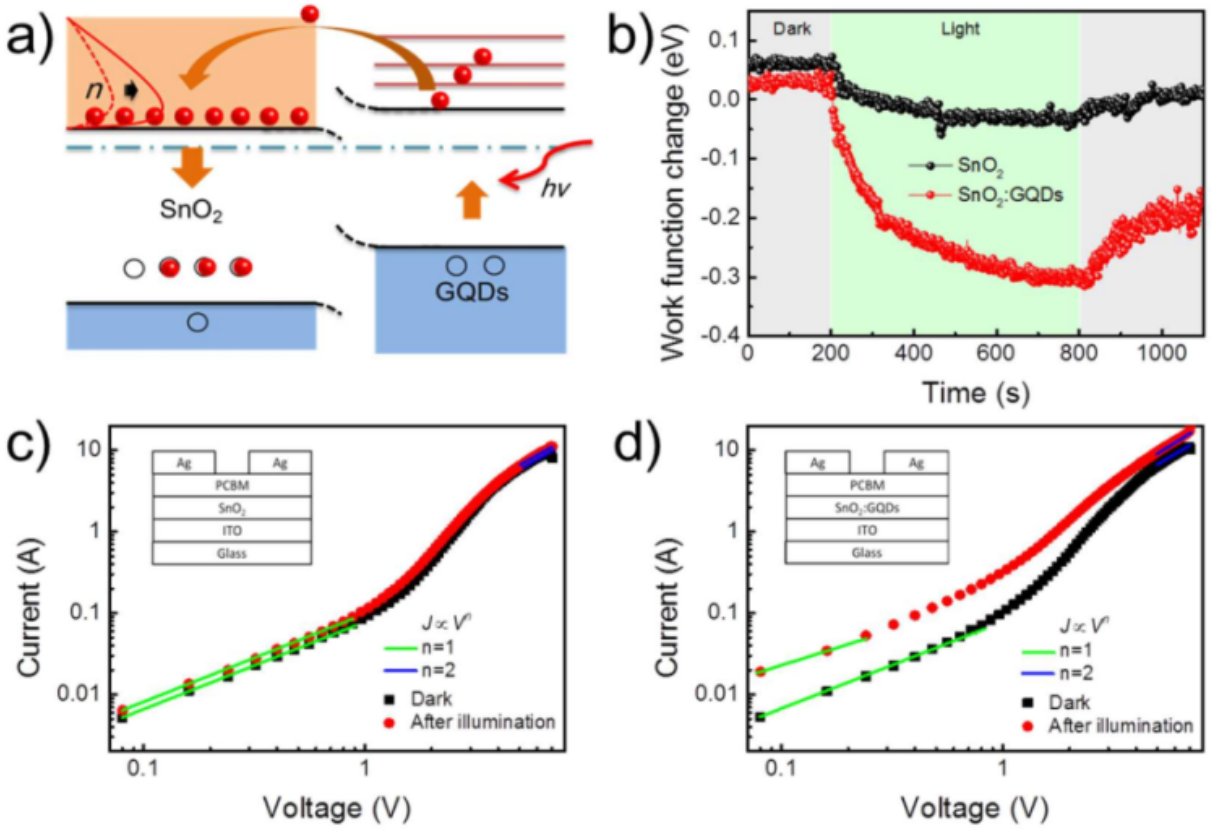

Figure 13. (a) A schematic of the hot electron transfer from GQDs to SnO_2 under illumination. b) Work function change of the SnO_2 and SnO_2 (c) Electron traps and mobility of SnO_2 and d) SnO_2: GQDs determined by the space-charge-limited current (SCLC) method. Copyright (2017) American Chemical Society.[52] *Reprinted with Permission.*

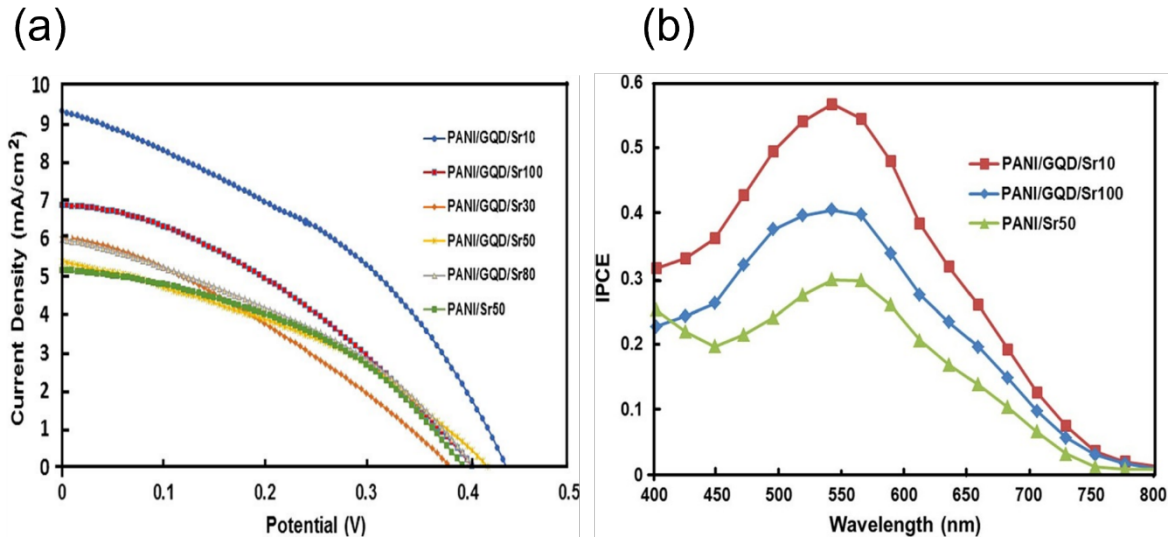

Figure 14. (a) Photocurrent density–photovoltage (J–V) curves of DSSCs using PANI and PANI–GQD counter electrodes prepared with different scan rate (b) Comparison of IPCE spectra of PANI and PANI–GQD photocathode based on DSSCs. Copyright (2016) Springer.[59] *Reprinted with Permission.*

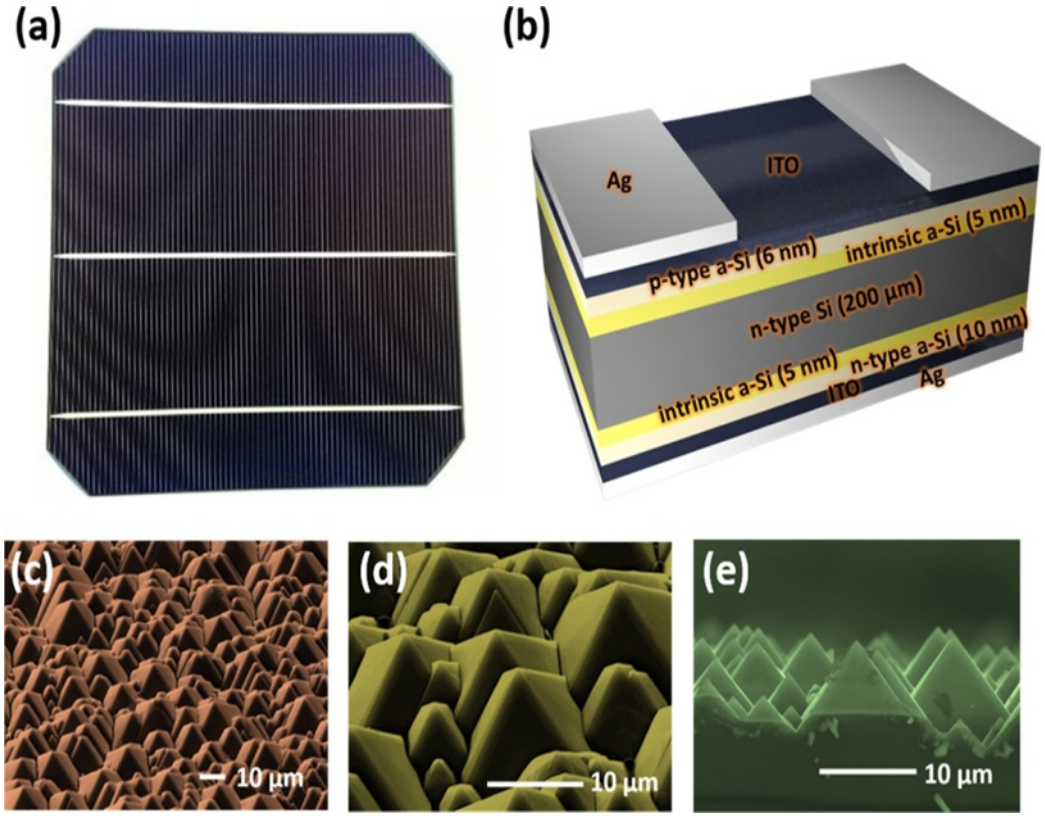

Figure 15. (a) Photographic image, (b) schematic, (c) low-resolution, (d) high-resolution, and (e) cross-sectional SEM images of SHJ solar cell. Copyright (2016) American Chemical Society[64]. Reprinted with Permission.

and UCPL emission is a critical parameter for LSCs[68]. The layer of GQDs that acts as the LDS layer increases the J_{SC} of mc-Si and c-Si photovoltaic cells by 5.14 % to 6.82 %, respectively. Remarkable relative enhancements in short circuit current density under ultra violet lightning revealed that the luminescent down shift layer boosts short circuit current density via decelerating effect. The use of a luminescent down shift layer has been presented as a strategy to increase photovoltaic cells' spectrum responsiveness[69]. Because of the small PL QY or Stokes switch; most of the GQDs are unsuitable as down-converting Copper Indium Gallium Selenide cells. Khan, F., and J.H. Kim used a newly developed approach to adjust the doping concentration as well as the N and O constituents, resulting in Nitrogen-doped GQDs with an amazingly high PL QY and a substantial Stokes switch[70]. GQDs have also enhanced the efficiency of PSCs. Because of its weak film-forming ability and low work function, graphene oxide is unsuitable for PSCs. F-GQDs can be utilized in solar cells with maximum reliability as hole-extraction surface[71]. GQDs were used to increase the functionality of inverted bulk heterojunction (BHJ) PSCs by acting as a cathode shield additive. The PCE of GQDs–Cs_2CO_3-based instruments are enhanced. This is because the cathode/polymer active layer interface has improved free charge recombination which was reduced due to excitation dispersion PCBM has a high cycle of[6,6] phenylC61-butyric acid methyl ester and a wide bandgap which is 3.7 eV[72]. A global evaluating model that depicts the micro-mechanism of improved molecular photoelectric performances by importing GQDs was created by Zhao, D., et al. The photo current-voltage evaluating a model for GQDs can serve as a foundation for evaluating nanomolecular photoelectric performance[73]. Moreover, GQDs were investigated by Archana, T., et al. as a passivating film for quantum dot-sensitized solar cell (QDSCs) containing cadmium sulfide (CdS). Under similar conditions, the photo conversion efficiency of QDSSC is up to 25% which is greater than that of comparable cells. GQDs have a high passivating layer efficacy over a CdS-loaded titanium dioxide (TiO_2) photo anode[74].

Li/Na batteries

Emerging energy issues arising from ever-increasing population and the usage of crude oil, which increased CO_2 levels, have driven attempts to reach fill-in renewable energy, specifically ones that are gathered naturally and require storage devices. As a result, potent, extended cycling life, high com-

Table 1. Power conversion efficiency of different types of solar cells is affected by doped GQDs.

Type of Solar Cells	Doped GQDS improvised in solar cells	Increase in PCE	Impact of inserting GQDs in solar cells	
Reversed flexible perovskite solar cell	A-GQDs	Increased up to 18%	Increased band structure in between HTL and perovskite monolayer	50
Inorganic γ-CsPbI3 Perovskite Photovoltaic Cells	N-GQDs	16.02%	The JSC increased significantly	51
Planar PSCs	SnO2: GQDs ETLs	20.23%	Maximum steady-state efficiency was obtained	52
FAPbI3 plane perovskites	I-GQDs	22.37%	Enhance ETL conductivity and energy level alignment, resulting in better interface carrier transfer	54
DSSCs	Boron-doped GQDs	3.7% higher	Boron-doped GQDs functioned as effective photoanode	58
SHJ photovoltaic cells	Down conversers GQDS	16.55%	The GQD effect allows for more photons to be absorbed in the depletion region, resulting in a stronger photovoltaic effect	64
BHJ solar cells	Reduced GQDs	From 6.70% to 7.60%	GQDs play a crucial function in charge carrier separation and improving visual absorption rate	66
CIGS solar cell	NGQD	15.31%	The down conversing of photon and light-capturing effect induced by using the NGQD enhanced the efficiency of power conversion	70
PSCs	F-GQDs	7.9%	F-GQDs can be utilized in solar cells with maximum reliability as hole-extraction layer	71
Inverted BHJ PSCs	GQDs–Cs2CO3	22%	GQDs were used to enhance the functionality by acting as a cathode shield additive	72

pactness, smaller weight, and high stability are all necessary. Due to their outstanding properties, Li/Na ion batteries (LIBs/NIBs) considered having bright future [71].

Li-ion batteries

Transition metal oxides and sulfides have been well established as efficient bidirectional cathode materials, whereas graphite has been well recognized as anode materials, since the invention of portable power. To avoid safety hazards, it was chosen to employ a cathode of lithium transition metal oxide as it became accessible [75]. GQDs have excellent properties, such as their huge surface area and ease of operation, which are critical in enhancing battery performance. 2D QDs can be used to account for some of the inadequacies of traditional electrode materials, including low conductivity and instability. Being a potential cathode for LIBs, Chao et al. harvested VO_2 nanobelts assembling coated with 3D graphene. Possessing a current density of 1/3 Coulomb, they have successfully increased the specific capacity of 421 $mAhg^{-1}$, increased rate performances, and 99.0 % faradaic yield. The distinct nanostructure helps to eliminate the need for binders (PVDF, PTFE, etc.) and reduces the cell's overall weight. The active material is protected from forming a solid-layer interface (SEI) by GQDs, leading to enhanced Columbic efficiency. Figure 16 depicts the fabrication procedures for the array of GF-supported GQD-coated VO2 nanobelts. [76]. Tian, L., et al., reported coating of the GQD layer on VO_2 increased the oxide's electrical conductivity, while also protecting the active substance from aggregation and disintegration. GQDs also made the oxide surface lipophilic, allowing for better ionic/electrolyte transport and improved chemical kinetics. At last, the nanocavities generated by assembled GQDs preferred Li+/Na+ ion transit pathways and also provided higher capacities via surface assimilation between GQDs and Li+/Na+ ions, resulting in greater capacities [77]. Zhang et al. assembled hierarchical TiO_2 embedded within GQDs, leading to an increased specific capacity of 160.1 $mAhg^{-1}$ at 10 C following 500 cycles [53]. Manikandan et al., showed that at all specific currents, boron-doped GQD has a greater specific capacity than nitrogen-doped GQD and GQD. The ability of boron-doped GQD, nitrogen-doped GQD and GQD to cycle for 500 cycles is inves-

tigated by sustaining a constant specific current of value 200 mAg^{-1}. After 500 cycles, B-GQD as a LIB anode holds 95.7 % of its original capacity, as N-GQD and GQD retain 90 and 86 %, respectively. All of the three LIB anodes exhibit a faradic yield of almost 100% over 500 cycles. Much relevant theoretical research has found that boron doping renders graphene an electron-deficient system, resulting in a significant increase in Li+ ion storage capacity sites[75]. Furthermore, according to Wang et al., single boron atom doped into the graphene matrix may absorb 6 Li+ ions, making it an effective lithium storage medium[78]. Manikandan, A., et al., reported that sulfur-doped carbon composites have piqued interest as a result of their improved rechargeable battery performance. For instance, the anode of MoS_2 doped graphene has a higher reversible capacity of 1290 $mAhg^{-1}$. Even though MoS_2 is a highly desirable material, significant volume elevation, annihilation, and assemblage of MoS_2 compromise the active material in LIB.

Thus, after the doping of GQDs, the competition between the photogenerated exciton and the charged exciton caused by a transfer of charge at 0D/2D multi-layer intersection results in unusual PL[75]. $Li_4Ti_5O_{12}$ (LTO) Nano sheets embedded with MoS_2 QD were fabricated by Xu et al., They inferred these nanosheets had great capacity, high rate potential, and outstanding cycling balance. Following 20 cycles, the hetero-structure composite displays a consistent reversible specific capacity of 170 $mAhg^{-1}$, which is obtained at 160 mA after thousand cycles at an increased rate of about 10 C, in the company of 94.1 % durability[79]. CuO/Cu/GQD triaxial nanowire alignments such as electrode materials for lithium-ion batteries were first described by Zhu et al. in 2004 (LIBs)[80]. The layer of GQDs coated on CuO/Cu is done to prevent the formation of SEI (solid electrolyte interface) on the active material. This is to improve the chemical kinetics by reducing its electrochemical impedance. As a result, during 500 cycles at one-third of C (1 C = 674 mA g^{-1}), the CuO/Cu/GQD electrode demonstrated a starting discharge capacity of about 960 $mAhg^{-1}$, a starting faradaic efficiency of about 87 %, along with a greater reversible specific capacitance of 780$mAhg^{-1}$ [80]. T. Hou et al., devised a covalent coupling technique for anode materials based on transition-metal sulfide (TMS) by using an amide linkage to combine the TMSs along with CNTs (carbon nanotubes). The composite shows clear pseudo capacitive behavior as well as very reversible electrochemical processes because of the good coupling interaction between CNTs and ZnS, which results in greater protracted stability as well as outstanding rate capability, with reversible capacities of 333 $mAhg^{-1}$ at 2 A g^{-1} after 4000 cycles for LIBs and 314 $mAhg^{-1}$ at 5 Ag^{-1} after 500 cycles for SIBs. As a consequence, the technique of covalent coupling is thought to be a very useful way to develop highly efficient materials for the anode, besides that CC-ZnS/CNT have showed the exceptional capability to be used in LIBs and SIBs[81].

Na-ion batteries

Rechargeable Li-ion batteries (LIBs) have improved significantly in recent years and are now extensively applied in a variety of electronic devices, automobiles, and handy power. Even though the LIBs function commendably, these are expensive, short lifetime, lower productivity, and safety concerns[82–84]. Battery output is predicted to rise as a result of the diversity and widespread use of rechargeable batteries. As a result, sodium-ion batteries (NIBs) may be used to replace LIBs soon because the Na element is inexpensive, non-toxic, plentiful, and widespread on the planet[85,86]. On account of the small ionic radius and atomic weight of Na-ion, it can be fabricated into electrode materials[87,88]. Owing to graphene's exceptional transparency, various applications in other domains are possible. In addition; Xu et al. created graphene composites based on metal for fuel cell technology, and also showed graphene-enhanced cell efficiency[79]. According to Yan, Y., et al, the dimensional confinement of electronic states is a perfect aim to tune attributes of graphene along with selecting a perfect bandgap that can be changed by the insertion of specific ions or molecules[89]. To design acceptable graphene, an approach for manufacturing of graphene of a specified size must be developed[90,91]. Furthermore, Daryabari, S., et al suggested that the high-chemical-activity edge C-atoms in permeable graphene should be passivated. Increasing the conjugated system of the electrode material to create peculiar mechanical, electrical, electronic, and other exceptional features is one of the techniques in the molecular design strategy. Despite several investigations and advances in experimental tools for the creation of porous graphene, the structure-property link remains a mystery[92]. Shabnam D. et al. used first-principles simulations to compare graphene's four defects incorporated with H, N, and F. $Na@F_3H_3.Gr$ and $Na@F_3.Gr$ have electrical conductivities of 6.51 $\times 10^{13}$ and 5.26 $\times 10^{12}$, respectively. The strong HOMO/LUMO coupling of the F-doped GQDs with the Sodium appears to have facilitated the transmission of electric current and resulted in excellent electrical conductivity. The cell potential of F-doped defects is higher than that of N-doped defects. They revealed that various aspects go into making a better ion battery and that interpreting the data solely consisting of charge transfer is erroneous[92]. Sun, J., et al reported that Phosphorene can also function at very high voltages (up to B2.9 V). Phosphorene is thought to be prospective for Na-ion batteries, having a specific capacity of 865 $mAhg^{-1}$ NaP sodiation and 433 $mAhg^{-1}$ for NaP_2 sodiation. Sun et al.

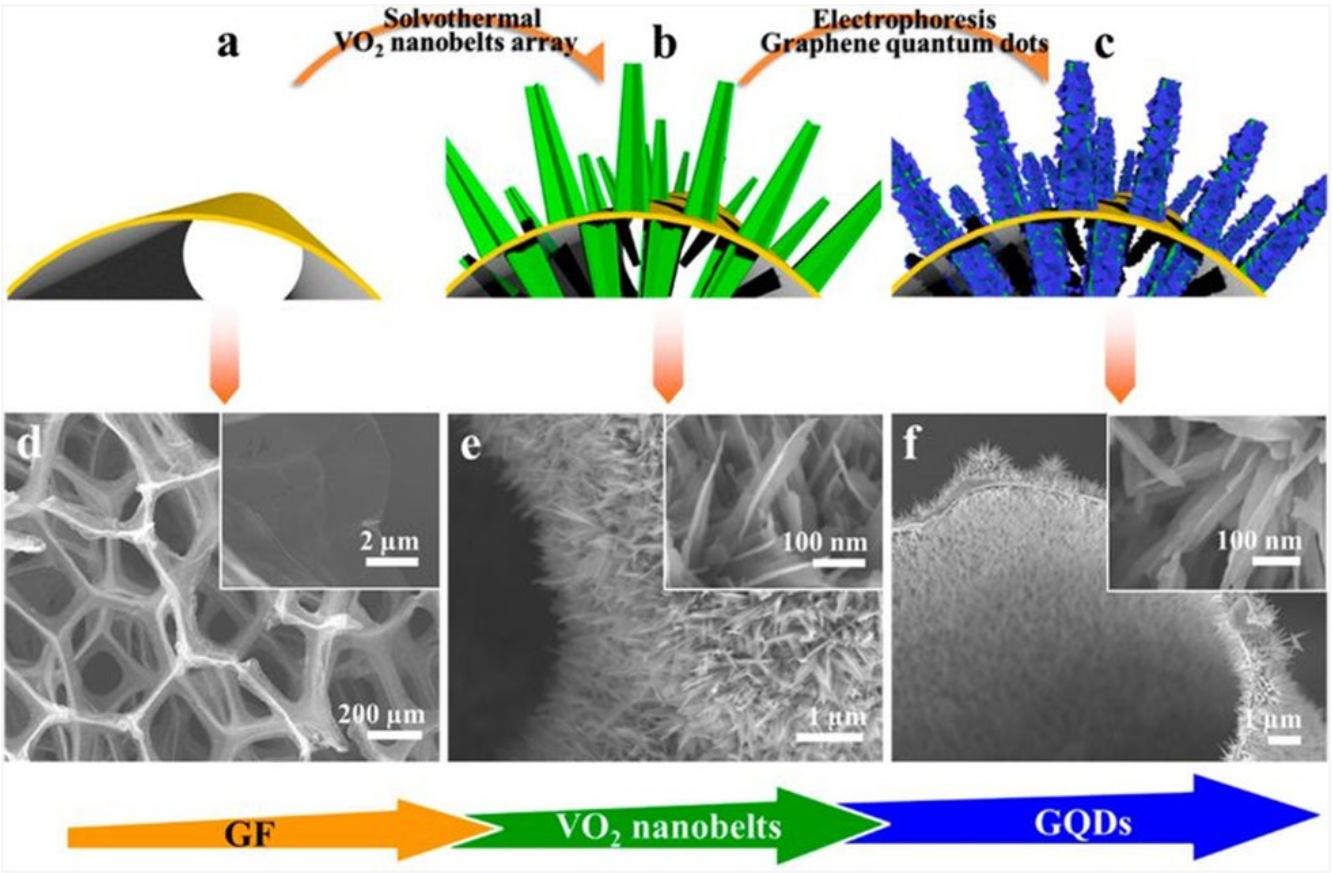

Figure 16. Fabrication processes of GF supported GQDs-coated VO2 nanobelts array. (a−c) Schematics of the fabrication process. The yellow basis represents the GF substrate. The green arrays represent VO2 nanoarrays, and the blue covering represents the GQDs. (d−f) The corresponding SEM images (fine structure in inset). Copyright (2015) American Chemical Society.[76] *Reprinted with Permission.*

developed an interlayer phosphorene–graphene hybrid cathode material for NIB that has an increased specific capacity of 2440 $mAhg^{-1}$ at a current density of about 0.05 Ag^{-1}. Furthermore, because of its greater active surface area and strong Na-ion storing capacity, current work on rising novel active material, GQDs has a critical role. With the voltage range of 3.5 to 1.5 V vs Na/Na, GQDs embedded on VO_2 nanobelts offer a higher discharge capacity of 306 $mAhg^{-1}$ at 1/3 C[93]. Moreover, because of the stipulated heterostructure, significant current densities can be charged and discharged. It has outstanding stability and capacity when cycled at a high speed. Furthermore, Hou, H., et al reported that after 1500 cycles at 60 C long-term instantaneous charge/discharge cycling yielded 88 % retention. The structural stability and pseudo capacitive behavior of VO_2 incorporated with GQDs contribute to its exceptional electrochemical performance, which features more efficient capability and long-term cycling tolerance[94]. Carbon-based quantum dots (CQDs) and derivative 3D highly porous carbon structures were reported by Hou et al. as having a high yield product. Based on the initial discharge and charge capacities, it is clear that the irreversible reaction, leads to formation of an SEI layer (735.1 and 255.5 $mAhg^{-1}$). Initial charge capacities of 255.6 $mAhg^{-1}$ are attained when the current density attains value of 0.5 and 2.5 Ag^{-1}. More sodium storage sites and a reduced Na diffusion length are provided by the 3D porous frameworks, resulting in improved performance[94]. Surprisingly, the MoS_2 implanted in lithium-titanium-oxide (LTO) exhibited a higher capacity of about 91 $mAhg^{-1}$ at a 5 C rate, as well as greater capacity retention of 10 $mAhg^{-1}$ following 200 cycles at 2 C reported by Xu, G., et al. The use of a 2D QD/LTO-based anode material for sodium-ion batteries (NIBs) improves rate capability, capacity, along with cycling stability, providing a framework for the operation of cost-effective alternative storage systems[79]. According to Tian et al., using 2-dimensional QDs in NIBs or LIBs minimized the mechanical stress caused by ion insinuation while also improving cycling stability and capacity[77].

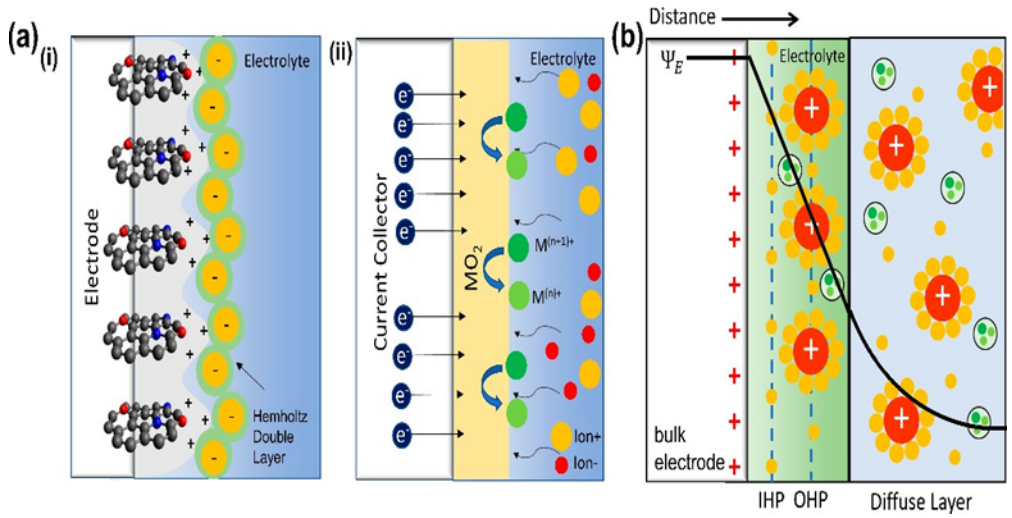

Figure 17. (a) Illustration of the Stern model for electrolyte ions on a charged electrode in (i) an electric-double-layer capacitor (EDLC) and (ii) a pseudo capacitance supercapacitor, as well as (b) a schematic model of ion distribution and mechanism.[96] *Reprinted with Permission.*

Supercapacitors

Energy crises and environmental risks are the most severe challenges. Energy storage devices need to meet high power density, high energy density, cost-effective, design environmental safety and long life cycle.[95] Supercapacitor devices are categorized in three categories depending upon their mechanism of storing electric charges: electric-double-layer capacitors (EDLCs), pseudo capacitors, and mixed supercapacitors.[96]

C-QDs have sparked enough interest due to their unique features[11]. In supercapacitor (SC) applications, mixing sulfide with transition metal is more useful in generating elevated pseudo-capacitive efficiency than transition metal oxide. However, they share the same problems as transition metal oxides, like restricted ease of electron transport and rapid capacity decay at rapid charging-discharging rates. Monghimian et al. claimed that a mixture of metal sulfide, for example, MoS_2, and GQD was able to reduce resistance at the electrode/electrolyte contact[97]. Moreover, according to Huang, Y., et al, the hollow structure produced by appropriate GQD synthesis helps limit any cracking during the cycling process, which is good for relaxing volume expansion.[98] The incorporation of GQDs into transition metal sulfide (TMS) or transition metal oxide (TMO) materials, according to Ganganboina, A.B., is largely aimed to boost the composite conductivity.[99] According to Hong, Y.et al, the incorporation of GQDs into a $Ni(OH)_2$/carbon fabric, as shown in Figure 18, the SC electrodes' conductivity effectiveness was improved as a result of this modification, allowing them to operate up to 2000 cycles. The increased electron conductivity was assumed to produce non-rectifying junction generation by $Ni(OH)_2$ because of the incorporation of GQDs[100] . The electrodes are made more flexible by the addition of GQDs, which depicts a further study of the GQDs/Ni $(OH)_2$, which shows that no particular changes in the cyclic voltammetry (CV) were reported with different bending angles.

According to Wang et al., as shown in Figure 19, layer-by-layer covering Carbon Fiber Cloth/polyaniline (CFC/PANI) alternating with GQDS/rGO on a layer of carbon improve electrode efficiency. As for this, GQD's job includes the improvement of the carbon layer's interactivity with the polymers by changing its hydrophobic character. Because of the powerful electrostatic contacts linking the PANI and GQD-rGO layers, self-assembled 3D structures are coherent. With increasing the current density, the capacitance of 20/CFC maintains at 89.7 %, which can be cycled at a quicker rate than some other alterations with the same starting capacitance. During the phenomenon of charge-discharge, PANI, being a pseudo-capacitive material, exhibit volumetric variation and residual stress. It was noted to be the reason for a slight drop in this material's capacitance. There's much less internal tension throughout the surgery since the PANI is incorporated via GQD-rGO[101] . According to Luo, J et al., due to the abundance of π-conjugation and edge sites in GQDs, $NiCO_2O_4$ characteristics like conductivity, surface area and thickness can be increased. The SC properties of other materials can be improved by utilizing the GQD edge features[102] . According to studies by S.N.J et al., GQDs/polymers with negative charge can provide oppositely charged ions on the upper surface of conductive polymer materials, allow-

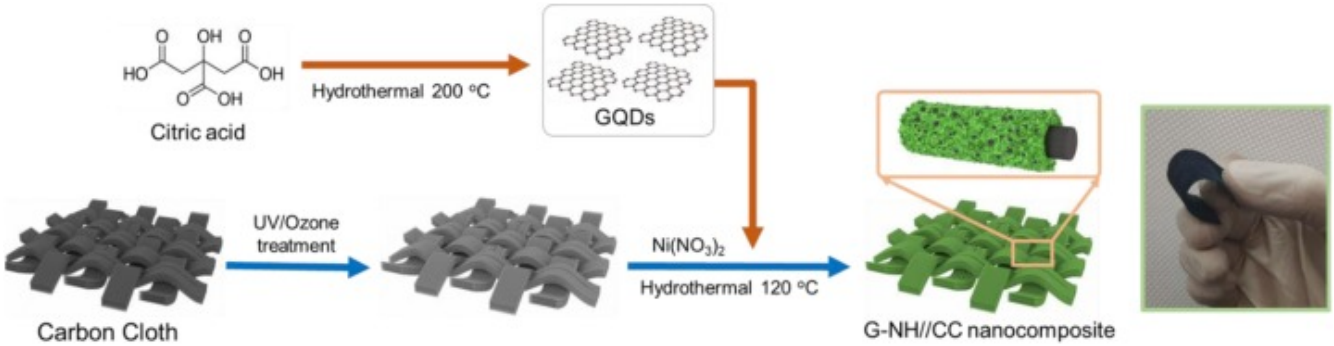

Figure 18. Figure 18: Schematic illustration for the synthesis of GQDs/Ni(OH)2 nanocomposite on carbon Cloth. Copyright (2020) Elsevier[100].

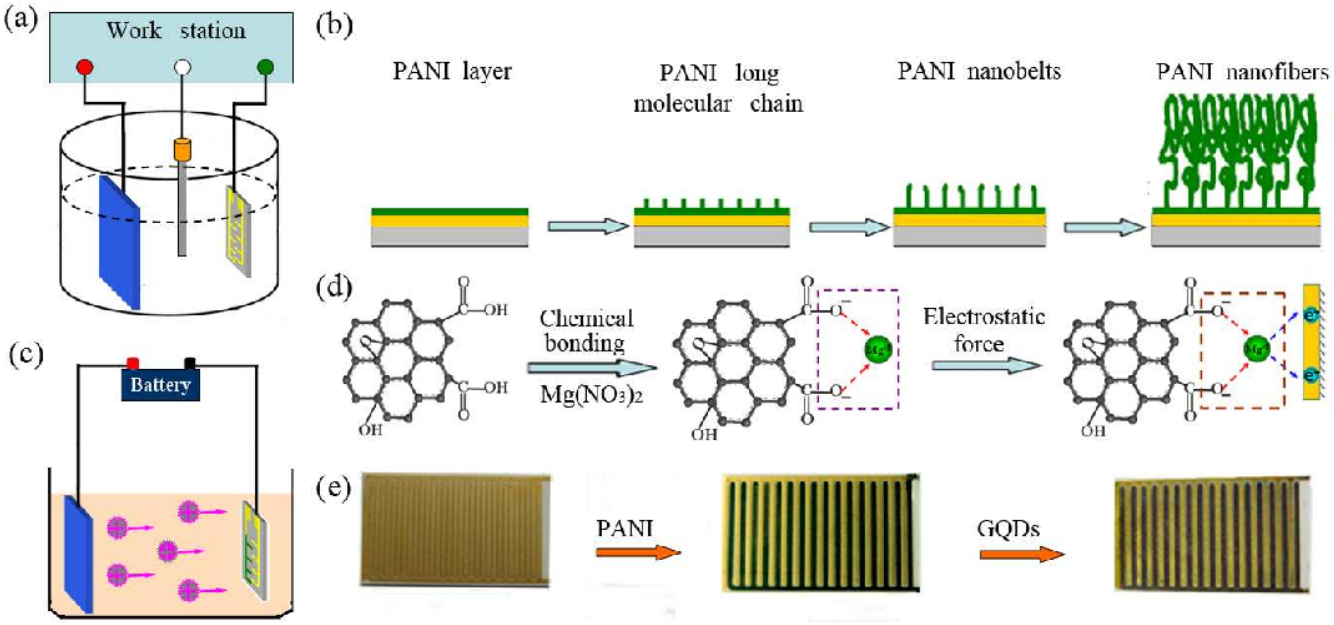

Figure 19. Schematic diagram of electrochemical depositions of PANI nanofibers, GQDs, and the structure of the device. Copyright (2013) Royal Society of Chemistry.[104] *Reprinted with Permission.*

ing the electrical double-layer phenomenon capacitor (EDLC) phenomena to improve the specific capacitance[103] .

As considered by Luo J et al., the SC properties of many other composites can be improved by utilizing the GQD edge features. Because GQDs have a lot of π-conjugation as well as edge sites, they can boost $NiCO_2O_4$ features like conductance, wet ability, and size distribution[102]. The peculiar uniform states of GQDs can serve as the host sites for the free electrons, such as those emitted by transition metals in the respective composites. Extra electrostatic attraction can be produced by free electrons accumulating at the edge, increasing the specific capacitance of established EDLs[105]. Li, Z et al., reported that fabricating GQDs to a MOF improves its wet ability. As a result, its specific capacitance increases. An asymmetric supercapacitor containing N-GQDs/cMOF can have a greater specific capacitance of 294.1 F g^{-1} at half (0.5) A g^{-1}. Through the pseudo capacitive characteristic of N-GQDs, this higher specific capacitance was a result of the outstanding electrochemical kinetics[60]. Another high conductivity polymer that has been coupled with GQDs and exhibited great SC performance is poly (3, 4-ethylenedioxythiophene): poly (vinyl alcohol) (PEDOT: PVA). Electro spinning was employed to build a basic assembly that encapsulates GQDs in PEDOT: PVA nanofiber. GQD's particle size may be reduced to a fraction of its original size using this approach, which is advantageous for supercapacitors. Adding GQDs to the polymer composite and transition metal sulfide synthesis process has a

second favorable effect on the generated materials. The GQDs may be able to regulate the anisotropic proliferation of the transition metal sulfide along with changed polymer's polarity, resulting in a nanoscale grouping of components [103]. Among the most important aspects of SC, device performance is electrode morphology. When Huang et al., mixed GQDs with $CuCo_2S_4$; they demonstrated that $CuCo_2S_4$'s morphology was improved by the inclusion of GQDs, making it more appropriate for a supercapacitor device with a rougher surface. During the synthesis process, adding GQDs to a composite might cause morphological alterations. After 10,000 cycles, GQDs/$CuCo_2S_4$ charge and discharge cycling performance demonstrates 90% capacity retention. As evaluated by electrochemical impedance spectroscopy, the efficient electron transfer rate resulted in a significant improvement in electrochemical performance (EIS) [106]. Another advantage of utilizing GQDs is the achievement of (metal-oxide-C) M-O-C covalent connection at intersection of the GQDs along with the hosts of metal oxide. MnO_2/GQDs manufactured with the help of metal-organic chemical vapour deposition (MOCVD) were discovered in order to feature M-O-C bonds that were discovered to be the source of improved capacity retention in the related SC devices [105,107,108]. Chang, H.-W. et al., claimed that MnO_2/GQDs successfully fabricated utilizing the metal-organic chemical vapor deposition (MOCVD) techniques were found to have M-O-C bonds, which were found to be the source of enhanced capacity retention in the associated SC devices. Some other studies found that the tight link between M-O-C and oxygen could operate as novel active sites for redox reactions [108]. According to Jia, H et al., many elements of supercapacitor electrodes can benefit from this type of heterostructure with M-O-C bonds [105]. Nonetheless, additional research into various metal oxide entities is advised. According to other investigations, introducing GQDs to the composite did not affect the morphology of $NiMoO_4$ [11]. Hence, some supercapacitor electrodes are not suited for C-QD composition. So we still need to be establishing certain ground rules.

LEDs:

The characteristics of GQDs, like possessing a tunable gap between the bands, high impressive optical and chemical stability, and biocompatibility make it, even more, a favorable material to be used in the optoelectronic field. The main reason for it is thought to be quantum confinement and edge effect [109]. In the light of these promising features, scientists have used GQDs to play several roles like electroluminescent phosphor, color converter as well as gap tuner, and a dopant [110]. Suk-Ho Choi vocalized in his article that organic LEDs in which GQDs were used to show the silvery emission of light as the current passed; having an external quantum efficiency of 0.1% However, the EL intensity shows a direct relationship with the GQD size, being kept at fixed bias. The reason behind this is the fact that the small bandgap of GQDs supports the energy transfer to GQD by a host. When the dimensions of GQD extended and its coordinates altered, the color emitted changed from blue to white. The blue LED was used to achieve white LEDs with a light conversion efficiency of almost 61.1% with the tendency to stay firm after being operated on for hours [111]. In an attempt to create LEDs with better quantum yield, Roy, P. et al., used organic plant leaves' extract of fenugreek and Neem to create GQDs of sizes 7 nm and 5 nm, without needing to use any kind of organic solvent or reducing agent. These GQDs were used to create a silvery luminance conversion cap using the RGB (red green blue) color mixing approach. Roy, P. et al., used two-step methods to construct an RGB gadget. To initiate, an N-GQD–QS–CPY mixture was created by combining emerald color PL emerging N-GQDs, azure color PL emerging QS, and ruby color PL emitting CPY solutions in PMMA at optimum ratios of 1:2, and 5:5. Second, as shown in Figure 20, the N-GQD–QS–CPY mixture was applied to a lab-made PET cap and allowed to dry overnight. After that, the cap was attached to a close Ultra Violet LED. These close-to-UV rays travel higher, and color changes because of electron transfer between the free spaces of bands when the electrons are excited. Few rays of UV, out of all, get soaked by the N-GQD-QS-CPYA center while some get past it, further out, and produce silvery luminance. The reason why color change occurs depends upon the electrons and their transitional behavior when they get excited in the band gap [112].

You Xiao Chen provided us with the stable bluish-emerald luminance emitting GQDs. By using the fullerene process and avoiding the usage of acid, he extracted ocherous color GQDs. These DGQDs along with the GQDs were also mixed with alcohol (PVA) to create see-through films of photoluminescence with outstanding elasticity as well as a preferred silvery light effusion quality that fit the needs of mercenary bright ivory Light Emitting Diodes [113].

Tetsuka et al., fragmented GQDs along with various nitrogenous groups, like ammonia, red p-methyl, 2, 3-naphthalenediamine, and azo compounds, to name a few [114]. GQDs that contain different nitrogenous groups have been discovered to be extremely different from each other in terms of the wavelength of their light emitted as well as their quantum efficiencies of luminance. The height of emission of 2, 3-naphthalenediamine improvised GQDs is moved to red light to 610 nm, whereas the GQDs treated with azo compounds gave out bluish-emerald luminance. Meanwhile, when compared to untreated GQDs, its fluorescence quantum efficiency is significantly higher. The PL spectra of D-GQDs at various excitation wave-

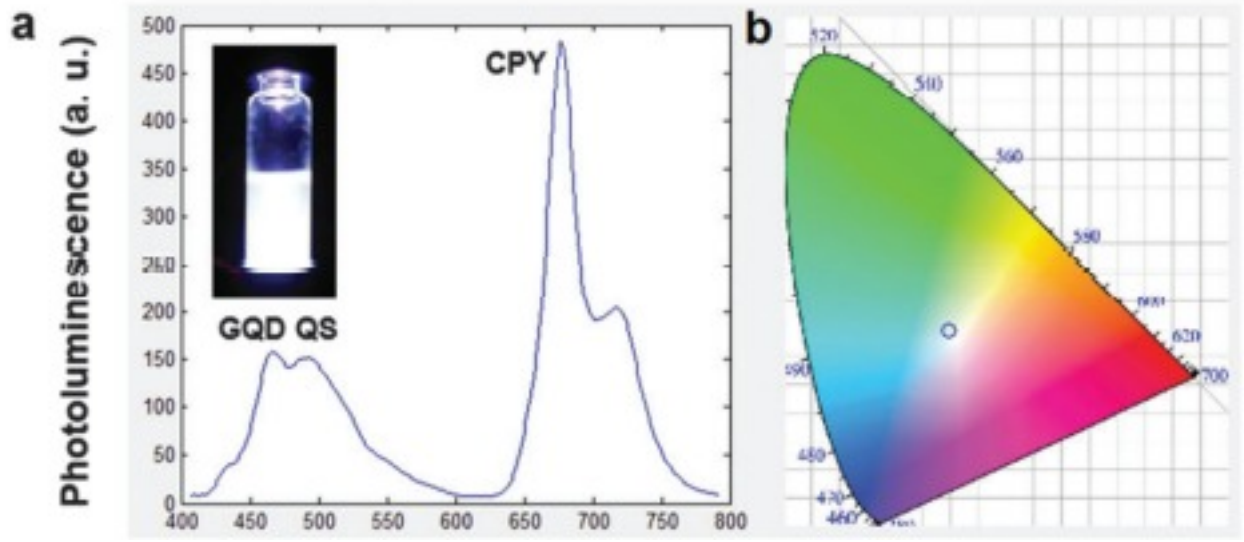

Figure 20. (a) PL spectrum of the N-GQD–QS–CPY coated PET cap (inset: photograph of the N-GQD–QS–CPY solution exhibiting white PL upon excitation using near-UV LED light). (b) Corresponding CIE spectrum when excited using near-UV LED light. Copyright (2014) Royal Society of Chemistry.[112] *Reprinted with Permission.*

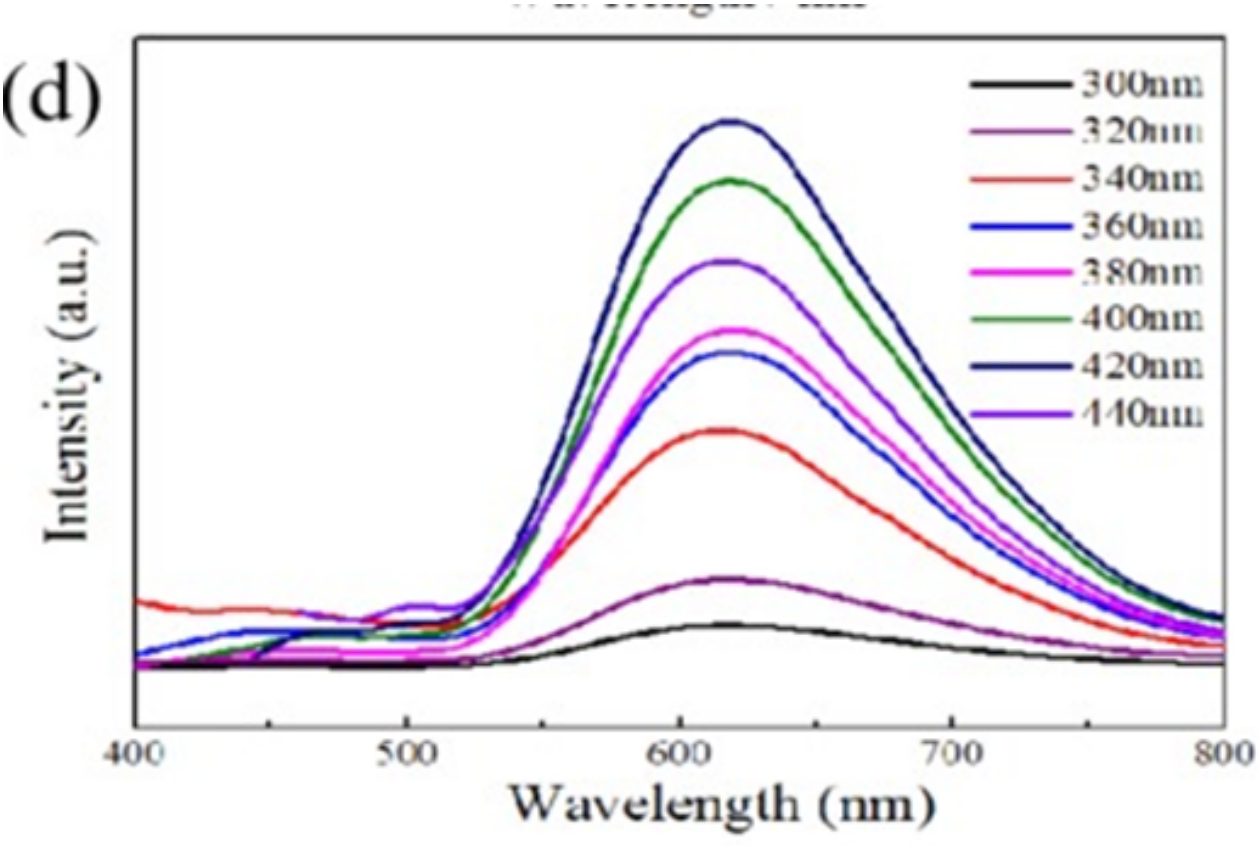

Figure 21. PL spectra of D-GQDs at different excitation wavelengths. Copyright (2020) American Chemical Society.[113] *Reprinted with Permission.*

lengths are shown in Figure 21[113]. GQD-based organic LEDs have lately made substantial progress. Gupta et al., suggested an interesting strategy for decreasing the initial voltage from approximately 6 V to 4 V by adding the two solutions that are GQDs with Methylene blue and 2-methoxy-5-(2-ethylhexyloxy)-1,4 phenylenevinylene (MEH-PPV). They also reported an increase in internal quantum efficiency after introducing GQDs. This improvement could be attributed to the increased presence of electrical conduction channels provided by GQDs. Charge injection in the active zone of the LED was facilitated by efficient electrical transit, resulting in a higher carrier depth. This Light Emitting device was more efficient with a non-high initial voltage[115]. Kwon et al., reported that amidative cutting of brittle graphite yields size-controlled GQDs (GQDs). With this approach, GQD sizes can be varied from 2 to more than 10 nm by varying the amine concentration. The energy gaps in such GQDs decreased as they grow in size resulting in vivid photoluminescence ranging from blue to brown. Moreover, they also showed that defect sites contribute to photoluminescence, long-wavelength emission, and a reduction in the lifetime of excitons successfully rendering white light with about 0.1 % external quantum efficiency[116]. Zhang et al., published a fascinating paper that demonstrated the development of electroluminescence from indigo to ivory light with various operating voltages. More study is required to increase various combinations of metals along with graphene and carbon QDs and build LED devices with improved performance[109]. Using octadecyl amine (ODA)-GQDs, Kim et al., generated solution-processed and extremely efficient LEDs. Nucleophilic substitutions between epoxy and amine functional groups were subjected to lower the quantity of O_2 in ODA-GQDs, when treated with simple GQDs. The efficiency of the current of ODA-GQDs was found to be 6.51 cd/A which is the highest among GQD-based LEDs that are previously reported. After a while, the group used edge functionalized GQDs (EF-GQDs) manufactured by an unusual mixture technique to create ultrahigh-luminosity white LEDs (WLEDs). The CIE coordinates and fluorescence for White color Light Emitting Diodes made from EF-GQDs were better than other WLEDs made from GQDs[117]. Kumar et al., have created WLEDs with phosphors made from ZnO films and GQDs. When compared to typical yellow phosphor WLEDs, UV-stimulated ivory light-emitting gadgets based on ZnO/GQDs are more appropriate for illumination[118]. In a single-step process, Kumar et al., showed how to synthesize the H_2O resistant GQDs in the powdered form in the absence of extreme pressure to make them useful in manufacturing LEDs. The current-voltage properties of GQD improvised LED devices revealed a below-average initial voltage of less than 2.5 V. An electroluminescence depending upon bias is exhibited, resulting in changing color from azure to deep cyan[119].

Under single-wavelength excitation, GQDs with amino-functionalized (afGQDs) produced with the help of a sheet of graphene, shine brightly with diverse hues, based on the functional groups. Resulting flexible afGQDs@CNF–clay sheets showed brilliant flamboyant fluorescence and were used as a color conversion substance for azure LEDs to create emission of ivory light[120]. Jung Kyu Kim1 et al., developed polymer light-emitting diodes (PLEDs) using GQDs. By using a modified hydrothermal oxidation process, the graphene oxide quantum dots were obtained which were treated with PVK to be used as an emissive surface to characterize the performance of PLED. The main reason for using ordinary, less complicated devices was to express the origination of luminance without the interruption of factors like impurity from other layers. The separate effusion of PVK and GOQDs contributed to the hybridized GOQDs-PVK emission which is mainly the reason for emission of silvery light[121]. Woosung Kwon et al., show that chemically functionalizing GQDs with aniline derivatives yields new energy levels, resulting in photoluminescence with exceptionally narrow line widths. Emerald, orange and crimson electroluminescent (LEDs) with great color purity were made by taking these functionalized GQDs in place of luminophores. This aniline derivative functionalization of GQDs is a new way of fabricating LEDs that create natural color[122].

GQDs having ivory luminance are manufactured utilizing a microwave-assisted hydrothermal technique where graphite is taken as precursor, according to Zhimin Luo et al., To make a solution-processed white-light-emitting diode, ivory luminance GQDs doped 4, 4-bis (carbazol-9-yl) biphenyl are employed as the emissive layer (WLED). The WLED with a ten % WGQD doping concentration generates white light. This show WGQDs, as a novel phosphor, could be proved useful for preparation of ecofriendly WLEDs, useful in solid-state lighting[31]. Dae Hun Kim et al., identified various flaws in GQDs that limit their fluorescence quantum yield, causing a reduction in the luminance of GQD-based light-emitting diodes (LEDs). He announced the development of solution-processed, high-efficiency LEDs based on octadecylamine (ODA)- Graphene Quantum Diodes. The well-to-do proof of this coherence efficiency increase for ODA-GQD-based LEDs suggests that GQD-based LEDs could be used as future better optical products[117]. Yin, L et al., showed the method of preparing dull-white lemon-greenish color effusing GQDs by using a process that is not only modest but also less complicated and non-toxic to the environment. Targeted Graphene nanoparticles were cast in UV- durable sili-

cone. A fine film of polymer, having properties like better transparency, was produced. The broadness of the film was tuned along with the GQDs congregation of color control matrix; the result appeared to be the formation of silver LEDs with changeable color temperatures. The CIE coordinates of the ivory light-emitting device based on GQDs were found to be perfectly linked with blackbody radiation curve. Admirable effusion and satisfaction could be attained using the fluorescent polymeric matrix in ivory Light Emitting gadgets[15,105]. PEG surface passivation was used to make blue-photo luminescent polyethylene glycol GQDs (PEG-GQDs) by Kim, H. J et al., PEG-GQDs with 320 nm excitation had a photoluminescence quantum yield (QY) of roughly 4.9 %. PEG-GQDs, which are highly fluorescent, will enable novel gadgets[120]. Tzu-Neng Lin et al., prepared 3.5 nm-sized GQDs via pulsed laser ablation which proved to be quite useful to achieve the enhancement of EL also a downfall was noticed in the series resistance of light emitting diodes. The amount of GQDs involved is found to be directly proportional to the emitted light[123]. C.M.Luk et al., presented an article revealing the production of GQDs that are soluble in water by using a way to make GQD composite with agar. The progress to be noted was that it had better optical stability and there was no luminance quenching. This composite was used as color-changing stuff in bluish LEDs, so that ivory lights can be achieved with luminance efficiency[124].

CONCLUSIONS

In this review, we have explored how unique optical and electronic properties of GQDs can benefit a verity of devices and applications. Mass manufacture of GQDs is crucial for their use in numerous industries. As many synthetic techniques for synthesizing GQDs have been developed so far, where oxidative cleavage of carbonaceous materials is most widely used to achieve mass production but post-processing is complicated to achieve. On the other hand, hydrothermal is ecofriendly, rapid and effective but the strong oxidation treatment of carbon materials before reaction makes it complicated. Also, microwave assistance methods can reduce the reaction time and enhance yield but are quite expensive to be carried on large scale. Additionally, the carbonization method is an environment-friendly and facile technique but the polydiversity of GQDs is the limitation to the method for industrial-scale production. We need to identify available commercially and efficient techniques to construct various GQDs for the further advancement of the GQDs. This review emphasizes the need for a relatively inexpensive and easy procedure, homogeneous products with desired specification, and higher yields. We have given a brief summary of several synthetic techniques for producing GQDs, as well as current energy-related uses of GQDs. Recent research on GQDs has increasingly been the focus of attention. Despite the rapid advancement, there are still concerns to be tackled and obstacles to overcome. GQD may be thought of as a complicated gigantic π-conjugated molecule, whose characteristics are controlled by a variety of parameters, including dimensions, functional groups, dopants, edge configuration, defects and structure. Without the ability to accurately manipulate GQD composition and shape, experimentally separating their effect is difficult, although theoretical investigations can give crucial insights. It is important to remember that GQDs made by various methods encompass a wide range of chemicophysical characteristics due to their considerable heterogeneity in composition, size, and form. As a result, an application that works with one type of GQD might not always work with another. To obtain better and more systematic characterization and comprehension of GQDs, as well as more successful applications, approaches to synthesizing GQDs with well-defined features, accurately engineering GQD attributes, or selectively separating various GQD populations are urgently needed. Many GQD applications are not practicable because low-cost industrial-scale manufacturing of GQDs has not yet been established. For instance, alternative techniques for mass production of GQDs of extended absorption spectra are required to improve their photo luminance properties. It may also be possible to narrow the band gap by doping hetero-atoms, like electron-donating atoms, by increasing the degree of conjugation. In the future, it will be important to develop simple purification procedures to eliminate excess chemicals which have the potential to cleave the carbon - containing surface, as well as unique approaches to producing an ultrahigh production without removing any starting materials. To achieve homogeneous GQD characteristics, new ways of distinguishing GQDs of different sizes are required. Also, GQDs' high solubility is one of their most outstanding features, allowing them to be employed in all devices' fabrication steps. In conclusion, taking these problems into account and applying the specific benefits of GQDs to industrial-scale applications will garner the ultimate value of GQDs. In the process of collaborating with researchers, we hope that new GQD preparation methods and attributes, as well as new gadgets and applications, will be discovered.

References

1) Rao, C. N. R.; Biswas, K.; Subrahmanyam, K. S.; Govindaraj, A. Graphene, the new nanocarbon. *Journal of Materials Chemistry* **2009**, *19* (17), 2457–2457.
2) Ren, W.; Cheng, H.-M. The global growth of graphene. *Nature Nanotechnology* **2014**, *9* (10), 726–730.
3) Kouwenhoven, L.; Marcus, C. Quantum dots. *Physics World* **1998**, *11* (6), 35–40.
4) Amiri, G. R.; Fatahian, S.; Mahmoudi, S. Preparation and Optical Properties Assessment of CdSe Quantum Dots. *Materials*

Table 2. Effect of doped GQDs on LEDs

Use of GQDs and doped GQDs	Improvement in efficiency of LEDs	Ref.
Organic plant leaves extract of fenugreek and Neem	Quantum yield became higher up to 38.9% and 41.2%	112
Fullerene process	Quantum yield increased upto 52.4 % peak of emission of 617 nm was obtained	113
GQDs act as dopant in CBP host	Successfully rendering white light with about 0.1 % external quantum efficiency	116
Quantum dots (GQDs) under microwave irradiation in 3 minutes (MA-GQDs)	Quantum yield and temperature increases to 35% and 4098 K	125
Octadecylamine (ODA)-GQDs	High efficiency of current of ODA-GQDs (6.51 cd/A) was obtained	117
GQDs mixed with aniline derivatives	Maximum current efficiency of 3.47 cd and external quantum coherence of 1.28% is obtained	122
GQDs doped with 4,4-bis(carbazol-9-yl)biphenyl	Light of brightness 200 cd m^2, voltage of 11–14 V and quantum productivity of 0.2% is obtained	31
Octadecylamine (ODA) mixed with Graphene Quantum	High-efficiency LEDs of quantum efficiency of 2.6 and efficiency of current is 6.51 cd/A is obtained	117
Polyethylene glycol mixed with GQDs	Quantum yield (QY) of roughly 4.9 % was obtained	120
GQDs via pulsed laser ablation	EL enhanced, series resistance decreased. Output light power of 71% is obtained	123
GQD composite with agar	There was no luminance quenching , luminance efficiency of 42.2 lmW^{-1} and 61.1% light conversion efficiency	112

Sciences and Applications **2013**, *04* (02), 134–137.

5) Vdovin, E. E.; Levin, A.; Patanè, A.; Eaves, L.; Main, P. C.; Khanin, Y. N.; Dubrovskii, Y. V.; Henini, M.; Hill, G. Imaging the Electron Wave Function in Self-Assembled Quantum Dots. *Science* **2000**, *290* (5489), 122–124.
6) Zrenner, A. A close look on single quantum dots. *The journal of chemical physics* **2000**, *112*, 7790–7798.
7) Zhang, Z.; Zhang, J.; Chen, N.; Qu, L. Graphene quantum dots: an emerging material for energy-related applications and beyond. *Energy & Environmental Science* **2012**, *5* (10), 8869–8869.
8) Ramezani, M.; Alibolandi, M.; Nejabat, M.; Charbgoo, F.; Taghdisi, S. M.; Abnous, K. Graphene-Based Hybrid Nanomaterials for Biomedical Applications. *Biomedical Applications of Graphene and 2D Nanomaterials* **2019**, 119–141.
9) Bacon, M.; Bradley, S. J.; Nann, T. 2014.
10) Tian, P. Graphene quantum dots from chemistry to applications. . *Materials today chemistry* **2018**, *10*, 221–258.
11) Bak, S.; Kim, D.; Lee, H. *Graphene quantum dots and their possible energy applications: A review* **2016**, *16*, 1192–1201.
12) Son, Y.-W.; Cohen, M. L.; Louie, S. G. Half-metallic graphene nanoribbons. *Nature* **2006**, *444* (7117), 347–349.
13) Jin, Z.; Owour, P.; Lei, S.; Ge, L. Graphene, graphene quantum dots and their applications in optoelectronics. *Current Opinion in Colloid & Interface Science* **2015**, *20* (5-6), 439–453.
14) Zhu, S.; Song, Y.; Wang, J.; Wan, H.; Zhang, Y.; Ning, Y.; Yang, B. Photoluminescence mechanism in graphene quantum dots: Quantum confinement effect and surface/edge state. *Nano Today* **2017**, *13*, 10–14.
15) Yin, L.; Zhou, J.; Li, W.; Zhang, J.; Wang, L. Yellow fluorescent graphene quantum dots as a phosphor for white tunable light-emitting diodes. *RSC Advances* **2019**, *9* (16), 9301–9307.
16) Zheng, P.; Wu, N. Fluorescence and Sensing Applications of Graphene Oxide and Graphene Quantum Dots: A Review. *Chemistry – An Asian Journal* **2017**, *12* (18), 2343–2353.
17) Wang, S.; Cole, I. S.; Li, Q. The toxicity of graphene quantum dots. *RSC Advances* **2016**, *6* (92), 89867–89878.
18) Tajik, S.; Dourandish, Z.; Zhang, K.; Beitollahi, H.; Van Le, Q.; Jang, H. W.; Shokouhimehr, M. Carbon and graphene quantum dots: a review on syntheses, characterization, biological and sensing applications for neurotransmitter determination. *RSC Advances* **2020**, *10* (26), 15406–15429.
19) Iravani, S.; Varma, R. S. Green synthesis, biomedical and biotechnological applications of carbon and graphene quantum dots. A review. *Environmental Chemistry Letters* **2020**, *18* (3), 703–727.
20) Facure, M. H. M.; Schneider, R.; Mercante, L. A.; Correa, D. S. A review on graphene quantum dots and their nanocomposites: from laboratory synthesis towards agricultural and environmental applications. *Environmental Science: Nano* **2020**, *7* (12), 3710–3734.
21) Li, K.; Liu, W.; Ni, Y.; Li, D.; Lin, D.; Su, Z.; Wei, G. Technical synthesis and biomedical applications of graphene quantum dots. *Journal of Materials Chemistry B* **2017**, *5* (25), 4811–4826.
22) Chen, W.; Lv, G.; Hu, W.; Li, D.; Chen, S.; Dai, Z. Synthesis and applications of graphene quantum dots: a review. *Nanotechnology Reviews* **2018**, *7* (2), 157–185.

23) Abbas, A.; Tabish, T. A.; Bull, S. J.; Lim, T. M.; Phan, A. N. High yield synthesis of graphene quantum dots from biomass waste as a highly selective probe for Fe3+ sensing. *Scientific Reports* **2020**, *10* (1), 1–16.
24) Pan, D.; Zhang, J.; Li, Z.; Wu, M. Hydrothermal Route for Cutting Graphene Sheets into Blue-Luminescent Graphene Quantum Dots. *Advanced Materials* **2010**, *22* (6), 734–738.
25) Zhao, C.; Song, X.; Liu, Y.; Fu, Y.; Ye, L.; Wang, N.; Wang, F.; Li, L.; Mohammadniaei, M.; Zhang, M.; Zhang, Q.; Liu, J. Synthesis of graphene quantum dots and their applications in drug delivery. *Journal of Nanobiotechnology* **2020**, *18* (1), 1–32.
26) Kalluri, A.; Debnath, D.; Dharmadhikari, B.; Patra, P. Graphene Quantum Dots: Synthesis and Applications. *Methods in Enzymology* **2018**, 335–354.
27) Tian, R.; Zhong, S.; Wu, J.; Jiang, W.; Shen, Y.; Jiang, W.; Wang, T. Solvothermal method to prepare graphene quantum dots by hydrogen peroxide. *Optical Materials* **2016**, *60*, 204–208.
28) Shen, J.; Zhu, Y.; Yang, X.; Li, C. Graphene quantum dots: emergent nanolights for bioimaging, sensors, catalysis and photovoltaic devices. *Chemical Communications* **2012**, *48* (31), 3686–3686.
29) Lu, J.; Yang, J.-X.; Wang, J.; Lim, A.; Wang, S.; Loh, K. P. One-Pot Synthesis of Fluorescent Carbon Nanoribbons, Nanoparticles, and Graphene by the Exfoliation of Graphite in Ionic Liquids. *ACS Nano* **2009**, *3* (8), 2367–2375.
30) Zhong, Y. L.; Swager, T. M. Enhanced Electrochemical Expansion of Graphite for in Situ Electrochemical Functionalization. *Journal of the American Chemical Society* **2012**, *134* (43), 17896–17899.
31) Luo, Z.; Qi, G.; Chen, K.; Zou, M.; Yuwen, L.; Zhang, X.; Huang, W.; Wang, L. Microwave-Assisted Preparation of White Fluorescent Graphene Quantum Dots as a Novel Phosphor for Enhanced White-Light-Emitting Diodes. *Advanced Functional Materials* **2016**, *26* (16), 2739–2744.
32) Zhang, M.; Bai, L.; Shang, W.; Xie, W.; Ma, H.; Fu, Y.; Fang, D.; Sun, H.; Fan, L.; Han, M.; Liu, C.; Yang, S. Facile synthesis of water-soluble, highly fluorescent graphene quantum dots as a robust biological label for stem cells. *Journal of Materials Chemistry* **2012**, *22* (15), 7461–7461.
33) Li, L.-L. L.; Ji, J.; Fei, R.; Wang, C.-Z.; Lu, Q.; Zhang, J.-R.; Jiang, L.-P.; Zhu, J.-J. A Facile Microwave Avenue to Electrochemiluminescent Two-Color Graphene Quantum Dots. *Advanced Functional Materials* **2012**, *22* (14), 2971–2979.
34) Ananthanarayanan, A.; Wang, X.; Routh, P.; Sana, B.; Lim, S.; Kim, D.-H.; Lim, K.-H.; Li, J.; Chen, P. Facile Synthesis of Graphene Quantum Dots from 3D Graphene and their Application for Fe3+ Sensing. *Advanced Functional Materials* **2014**, *24* (20), 3021–3026.
35) Naik, J. P.; Sutradhar, P.; Saha, M. Molecular scale rapid synthesis of graphene quantum dots (GQDs). *Journal of Nanostructure in Chemistry* **2017**, *7* (1), 85–89.
36) Tong, X.; Wei, Q.; Zhan, X.; Zhang, G.; Sun, S. The New Graphene Family Materials: Synthesis and Applications in Oxygen Reduction Reaction. *Catalysts* **2016**, *7* (12), 1–1.
37) Fresco-Cala, B.; Soriano, M. L.; Sciortino, A.; Cannas, M.; Messina, F.; Cardenas, S. One-pot synthesis of graphene quantum dots and simultaneous nanostructured self-assembly via a novel microwave-assisted method: impact on triazine removal and efficiency monitoring. *RSC Advances* **2018**, *8* (52), 29939–29946.
38) Alves, A. K.; Frantz, A. C. S.; Berutti, F. A. Microwave-assisted oleothermal synthesis of graphene-TiO2 quantum dots for photoelectrochemical oxygen evolution reaction. *FlatChem* **2018**, *12*, 26–34.
39) Tang, L.; Ji, R.; Cao, X.; Lin, J.; Jiang, H.; Li, X.; Teng, K. S.; Luk, C. M.; Zeng, S.; Hao, J.; Lau, S. P. Deep Ultraviolet Photoluminescence of Water-Soluble Self-Passivated Graphene Quantum Dots. *ACS Nano* **2012**, *6* (6), 5102–5110.
40) Zhang, C.; Cui, Y.; Song, L.; Liu, X.; Hu, Z. Microwave assisted one-pot synthesis of graphene quantum dots as highly sensitive fluorescent probes for detection of iron ions and pH value. *Talanta* **2016**, *150*, 54–60.
41) Yan, X.; Cui, X.; Li, L.-S. Synthesis of Large, Stable Colloidal Graphene Quantum Dots with Tunable Size. *Journal of the American Chemical Society* **2010**, *132* (17), 5944–5945.
42) Wang, L.; Li, W.; Wu, B.; Li, Z.; Pan, D.; Wu, M. Room-temperature synthesis of graphene quantum dots via electron-beam irradiation and their application in cell imaging. *Chemical Engineering Journal* **2017**, *309*, 374–380.
43) Shen, J.; Chen, W.; Yang, Z.; Lv, G.; Cao, J.; Li, D.; Liu, X. A Critical Review of Graphene Quantum Dots: Synthesis and Application in Biosensors. *Nano* **2021**, *16* (01), 2130001–2130001.
44) Dong, Y.; Shao, J.; Chen, C.; Li, H.; Wang, R.; Chi, Y.; Lin, X.; Chen, G. Blue luminescent graphene quantum dots and graphene oxide prepared by tuning the carbonization degree of citric acid. *Carbon* **2012**, *50* (12), 4738–4743.
45) Shen, C.; Ge, S.; Pang, Y.; Xi, F.; Liu, J.; Dong, X.; Chen, P. Facile and scalable preparation of highly luminescent N,S co-doped graphene quantum dots and their application for parallel detection of multiple metal ions. *Journal of Materials Chemistry B* **2017**, *5* (32), 6593–6600.
46) Allahbakhsh, A.; Bahramian, A. R. Self-assembly of graphene quantum dots into hydrogels and cryogels: Dynamic light scattering, UV–Vis spectroscopy and structural investigations. *Journal of Molecular Liquids* **2018**, *265*, 172–180.
47) Teymourinia, H.; Salavati-Niasari, M.; Amiri, O.; Safardoust-Hojaghan, H. Synthesis of graphene quantum dots from corn powder and their application in reduce charge recombination and increase free charge carriers. *Journal of Molecular Liquids* **2017**, *242*, 447–455.
48) Bayat, A.; Saievar-Iranizad, E. Synthesis of green-photoluminescent single layer graphene quantum dots: Determination of HOMO and LUMO energy states. *Journal of Luminescence* **2017**, *192*, 180–183.
49) Mishra, P.; Bhat, B. R. Synthesis and characterization of graphene quantum dots and their size reduction using swift heavy ion beam. *Radiation Effects and Defects in Solids* **2018**, *173* (3-4), 232–238.
50) Wang, Z.; Rong, X.; Wang, L.; Wang, W.; Lin, H.; Li, X. Dual Role of Amino-Functionalized Graphene Quantum Dots in NiOx Films for Efficient Inverted Flexible Perovskite Solar Cells. *ACS Applied Materials & Interfaces* **2020**, *12* (7), 8342–8350.
51) Bian, H.; Wang, Q.; Yang, S.; Yan, C.; Wang, H.; Liang, L.; Jin, Z.; Wang, G.; (frank) Liu, S. Nitrogen-doped graphene quantum dots for 80% photoluminescence quantum yield for inorganic γ-CsPbI3 perovskite solar cells with efficiency beyond 16%. *Journal of Materials Chemistry A* **2019**, *7* (10), 5740–5747.
52) Xie, J.; Huang, K.; Yu, X.; Yang, Z.; Xiao, K.; Qiang, Y.; Zhu, X.; Xu, L.; Wang, P.; Cui, C.; Yang, D. Enhanced Electronic Properties of SnO2 via Electron Transfer from Graphene Quantum Dots for Efficient Perovskite Solar Cells. *ACS Nano* **2017**, *11* (9), 9176–9182.
53) Zhang, J.; Tong, T.; Zhang, L.; Li, X.; Zou, H.; Yu, J. Enhanced Performance of Planar Perovskite Solar Cell by Graphene Quantum Dot Modification. *ACS Sustainable Chemistry & Engineering* **2018**, *6* (7), 8631–8640.
54) wen W Gao, Z.; Wang, Y.; Liu, H.; Sun, J.; Kim, J.; Li, Y.; Xu, B.; Choy, W. C. H. Tailoring the Interface in FAPbI3 Planar Perovskite Solar Cells by Imidazole-Graphene-Quantum-Dots. *Advanced Functional Materials* **2021**, *31* (27), 2101438–2101438.
55) Ahmed, D. S.; Mohammed, M. K. A.; Majeed, S. M. Green Synthesis of Eco-Friendly Graphene Quantum Dots for Highly Efficient Perovskite Solar Cells. *ACS Applied Energy Materials* **2020**, *3* (11), 10863–10871.
56) Shin, D. H.; Kim, J. M.; Shin, S. H.; Choi, S.-H. Highly-flexible graphene transparent conductive electrode/perovskite solar

cells with graphene quantum dots-doped PCBM electron transport layer. *Dyes and Pigments* **2019**, *170*, 107630–107630.
57) Shen, D.; Zhang, W.; Xie, F.; Li, Y.; Abate, A.; Wei, M. Graphene quantum dots decorated TiO2 mesoporous film as an efficient electron transport layer for high-performance perovskite solar cells. *Journal of Power Sources* **2018**, *402*, 320–326.
58) Kumar, M. P. Boron-doped graphene quantum dots: An efficient photoanode for a dye sensitized solar cell. *New Journal of Chemistry* **2019**, *43* (36), 14313–14319.
59) Dinari, M.; Momeni, M. M.; Goudarzirad, M. Dye-sensitized solar cells based on nanocomposite of polyaniline/graphene quantum dots. *Journal of Materials Science* **2016**, *51* (6), 2964–2971.
60) Ghayoor, R.; Keshavarz, A.; Rad, M. N. S.; Mashreghi, A. Enhancement of photovoltaic performance of dye-sensitized solar cells based on TiO2-graphene quantum dots photoanode. *Materials Research Express* **2018**, *6* (2), 025505–025505.
61) Chang, Q.; Ma, Z.; Wang, J.; Li, P.; Yan, Y.; Shi, W.; Chen, Q.; Huang, Y.; Huang, L. Hybrid Graphene Quantum Dots@Graphene Foam Nanosheets for Dye-Sensitized Solar Cell Electrodes. *Energy Technology* **2016**, *4* (2), 256–262.
62) Fang, X.; Li, M.; Guo, K.; Li, J.; Pan, M.; Bai, L.; Luoshan, M.; Zhao, X. Graphene quantum dots optimization of dye-sensitized solar cells. *Electrochimica Acta* **2014**, *137*, 634–638.
63) Zamiri, G.; Bagheri, S. Fabrication of green dye-sensitized solar cell based on ZnO nanoparticles as a photoanode and graphene quantum dots as a photosensitizer. *Journal of Colloid and Interface Science* **2018**, *511*, 318–324.
64) Tsai, M.-L.; Tu, W.-C.; Tang, L.; Wei, T.-C.; Wei, W.-R.; Lau, S. P.; Chen, L.-J.; He, J.-H. Efficiency Enhancement of Silicon Heterojunction Solar Cells via Photon Management Using Graphene Quantum Dot as Downconverters. *Nano Letters* **2016**, *16* (1), 309–313.
65) Gao, P.; Ding, K.; Wang, Y.; Ruan, K.; Diao, S.; Zhang, Q.; Sun, B.; Jie, J. Crystalline Si/Graphene Quantum Dots Heterojunction Solar Cells. *The Journal of Physical Chemistry C* **2014**, *118* (10), 5164–5171.
66) Kim, J. K.; Park, M. J.; Kim, S. J.; Wang, D. H.; Cho, S. P.; Bae, S.; Park, J. H.; Hong, B. H. Balancing Light Absorptivity and Carrier Conductivity of Graphene Quantum Dots for High-Efficiency Bulk Heterojunction Solar Cells. *ACS Nano* **2013**, *7* (8), 7207–7212.
67) Li, M.; Ni, W.; Kan, B.; Wan, X.; Zhang, L.; Zhang, Q.; Long, G.; Zuo, Y.; Chen, Y. Graphene quantum dots as the hole transport layer material for high-performance organic solar cells. *Physical Chemistry Chemical Physics* **2013**, *15* (43), 18973–18973.
68) Saeidi, S.; Rezaei, B.; Irannejad, N.; Ensafi, A. A. Efficiency improvement of luminescent solar concentrators using upconversion nitrogen-doped graphene quantum dots. *Journal of Power Sources* **2020**, *476*, 228647–228647.
69) Sabetghadam, S. A.; Hosseini, Z.; Zarei, S.; Ghanbari, T. Improvement of the current generation in silicon solar cells by utilizing graphene quantum dot as spectral converter. *Materials Letters* **2020**, *279*, 128515–128515.
70) Khan, F.; Kim, J. H. N-Functionalized Graphene Quantum Dots with Ultrahigh Quantum Yield and Large Stokes Shift: Efficient Downconverters for CIGS Solar Cells. *ACS Photonics* **2018**, *5* (11), 4637–4643.
71) Ding, Z.; Hao, Z.; Meng, B.; Xie, Z.; Liu, J.; Dai, L. Few-layered graphene quantum dots as efficient hole-extraction layer for high-performance polymer solar cells. *Nano Energy* **2015**, *15*, 186–192.
72) Yang, H. B. 2013.
73) Zhao, D.; Saputra, R. M.; Song, P.; Yang, Y.; Li, Y. How graphene strengthened molecular photoelectric performance of solar cells: A photo current-voltage assessment. *Solar Energy* **2021**, *213*, 271–283.
74) Archana, T.; Sreelekshmi, S.; Subashini, G.; Grace, A. N.; Arivanandhan, M.; Jayavel, R. The effect of graphene quantum dots/ZnS co-passivation on enhancing the photovoltaic performance of <scp>CdS</scp> quantum dot sensitized solar cells. *International Journal of Energy Research* **2021**, *45* (11), 15879–15891.
75) Manikandan, A.; Chen, Y.-Z.; Shen, C.-C.; Sher, C.-W.; Kuo, H.-C.; Chueh, Y.-L. A critical review on two-dimensional quantum dots (2D QDs): From synthesis toward applications in energy and optoelectronics. *Progress in Quantum Electronics* **2019**, *68*, 100226–100226.
76) Chao, D.; Zhu, C.; Xia, X.; Liu, J.; Zhang, X.; Wang, J.; Liang, P.; Lin, J.; Zhang, H.; Shen, Z. X.; Fan, H. J. Graphene Quantum Dots Coated VO2 Arrays for Highly Durable Electrodes for Li and Na Ion Batteries. *Nano Letters* **2015**, *15* (1), 565–573.
77) Tian, L.; Li, Z.; Wang, P.; Zhai, X.; Wang, X.; Li, T. Carbon quantum dots for advanced electrocatalysis. *Journal of Energy Chemistry* **2021**, *55*, 279–294.
78) Wang, X.; Zeng, Z.; Ahn, H.; Wang, G. First-principles study on the enhancement of lithium storage capacity in boron doped graphene. *Applied Physics Letters* **2009**, *95* (18), 183103–183103.
79) Xu, G.; Yang, L.; Wei, X.; Ding, J.; Zhong, J.; Chu, P. K. MoS2 Quantum-Dot-Interspersed Li4Ti5O12 Nanosheets with Enhanced Performance for Li- and Na-Ion Batteries. *Advanced Functional Materials* **2016**, *26* (19), 3349–3358.
80) Zhu, C.; Chao, D.; Sun, J.; Bacho, I. M.; Fan, Z.; Ng, C. F.; Xia, X.; Huang, H.; Zhang, H.; Shen, Z. X.; Ding, G.; Fan, H. J. Enhanced Lithium Storage Performance of CuO Nanowires by Coating of Graphene Quantum Dots. *Advanced Materials Interfaces* **2015**, *2* (2), 1400499–1400499.
81) Hou, T.; Liu, B.; Sun, X.; Fan, A.; Xu, Z.; Cai, S.; Zheng, C.; Yu, G.; Tricoli, A. Covalent Coupling-Stabilized Transition-Metal Sulfide/Carbon Nanotube Composites for Lithium/Sodium-Ion Batteries. *ACS Nano* **2021**, *15* (4), 6735–6746.
82) Prosini, P. P.; Cento, C.; Carewska, M.; Masci, A. Electrochemical performance of Li-ion batteries assembled with water-processable electrodes. *Solid State Ionics* **2015**, *274*, 34–39.
83) Slater, M. D.; Kim, D.; Lee, E.; Johnson, C. S. Sodium-Ion Batteries. *Advanced Functional Materials* **2013**, *23* (8), 947–958.
84) Er, D.; J, L.; M, N.; Y, G.; VB, S. Ti3C2 MXene as a high capacity electrode material for metal (Li, Na, K, Ca) ion batteries. *ACS applied materials & interfaces* **2014**, *6*, 11173–11179.
85) Palomares, V.; Serras, P.; Villaluenga, I.; Hueso, K. B.; Carretero-González, J.; Rojo, T. Na-ion batteries, recent advances and present challenges to become low cost energy storage systems. *Energy & Environmental Science* **2012**, *5* (3), 5884–5884.
86) Eslami, M.; Vahabi, V.; Peyghan, A. A. Sensing properties of BN nanotube toward carcinogenic 4-chloroaniline: a computational study. *Physica E: Low-dimensional Systems and Nanostructures* **2016**, *76*, 6–11.
87) Gao, S.; Shi, G.; Fang, H. Impact of cation–π interactions on the cell voltage of carbon nanotube-based Li batteries. *Nanoscale* **2016**, *8* (3), 1451–1455.
88) Mikhailov, S. In *Physics and applications of graphene: Experiments*; and others„ Ed.; BoD-Books on Demand, 2011.
89) Yan, Y.; Chen, J.; Li, N.; Tian, J.; Li, K.; Jiang, J.; Liu, J.; Tian, Q.; Chen, P. Systematic Bandgap Engineering of Graphene Quantum Dots and Applications for Photocatalytic Water Splitting and CO2 Reduction. *ACS Nano* **2018**, *12* (4), 3523–3532.
90) Neto, A. C.; F, G.; NM, P.; KS, N.; AK, G. *Reviews of modern physics* **2009**, *81*, 109–109.
91) Ullah, S.; Hussain, A.; Syed, W.; Saqlain, M. A.; Ahmad, I.; Leenaerts, O.; Karim, A. Band-gap tuning of graphene by Be doping and Be, B co-doping: a DFT study. *RSC Advances* **2015**, *5* (69), 55762–55773.
92) Daryabari, S.; Mansouri, S.; Beheshtian, J.; Karimkhani, M. A computational study on the novel defects of graphene quantum dot as a promising anode material for sodium ion battery. *Materials Chemistry and Physics* **2021**, *265*, 124484–124484.
93) Sun, J.; Lee, H.-W.; Pasta, M.; Yuan, H.; Zheng, G.; Sun, Y.; Li, Y.; Cui, Y. A phosphorene–graphene hybrid material as

a high-capacity anode for sodium-ion batteries. *Nature Nanotechnology* **2015**, *10* (11), 980–985.
94) Hou, H.; Banks, C. E.; Jing, M.; Zhang, Y.; Ji, X. Carbon Quantum Dots and Their Derivative 3D Porous Carbon Frameworks for Sodium-Ion Batteries with Ultralong Cycle Life. *Advanced Materials* **2015**, *27* (47), 7861–7866.
95) Chen, D.; Wang, Q.; Wang, R.; Shen, G. Ternary oxide nanostructured materials for supercapacitors: a review. *Journal of Materials Chemistry A* **2015**, *3* (19), 10158–10173.
96) Permatasari, F. A.; Irham, M.; Bisri, S.; Iskandar, F. Carbon-Based Quantum Dots for Supercapacitors: Recent Advances and Future Challenges. *Nanomaterials (Basel)* **2021**, 11–11.
97) Moghimian, S.; Sangpour, P. One-step hydrothermal synthesis of GQDs-MoS2 nanocomposite with enhanced supercapacitive performance. *Journal of Applied Electrochemistry* **2020**, *50* (1), 71–79.
98) Huang, Y.; Shi, T.; Zhong, Y.; Cheng, S.; Jiang, S.; Chen, C.; Liao, G.; Tang, Z. Graphene-quantum-dots induced NiCo2S4 with hierarchical-like hollow nanostructure for supercapacitors with enhanced electrochemical performance. *Electrochimica Acta* **2018**, *269*, 45–54.
99) Ganganboina, A. B.; Chowdhury, A. D.; Doong, R.-A. New Avenue for Appendage of Graphene Quantum Dots on Halloysite Nanotubes as Anode Materials for High Performance Supercapacitors. *ACS Sustainable Chemistry & Engineering* **2017**, *5* (6), 4930–4940.
100) Hong, Y.; Xu, J.; Chung, J. S.; Choi, W. M. Graphene quantum dots/Ni(OH)2 nanocomposites on carbon cloth as a binder-free electrode for supercapacitors. *Journal of Materials Science & Technology* **2020**, *58*, 73–79.
101) Wang, S.; Shen, J.; Wang, Q.; Fan, Y.; Li, L.; Zhang, K.; Yang, L.; Zhang, W.; Wang, X. High-Performance Layer-by-Layer Self-Assembly PANI/GQD-rGO/CFC Electrodes for a Flexible Solid-State Supercapacitor by a Facile Spraying Technique. *ACS Applied Energy Materials* **2019**, *2* (2), 1077–1085.
102) Luo, J.; Wang, J.; Liu, S.; Wu, W.; Jia, T.; Yang, Z.; Mu, S.; Huang, Y. Graphene quantum dots encapsulated tremella-like NiCo2O4 for advanced asymmetric supercapacitors. *Carbon* **2019**, *146*, 1–8.
103) Abidin, S. N. J. S. Z.; Mamat, S.; Rasyid, S. A.; Zainal, Z.; Sulaiman, Y. Fabrication of poly(vinyl alcohol)-graphene quantum dots coated with poly(3,4-ethylenedioxythiophene) for supercapacitor. *Journal of Polymer Science Part A: Polymer Chemistry* **2018**, *56* (1), 50–58.
104) Liu, W.; Yan, X.; Chen, J.; Feng, Y.; Xue, Q. Novel and high-performance asymmetric micro-supercapacitors based on graphene quantum dots and polyaniline nanofibers. *Nanoscale* **2013**, *5* (13), 6053–6053.
105) Jia, H.; Cai, Y.; Lin, J.; Liang, H.; Qi, J.; Cao, J.; Feng, J.; Fei, W. Heterostructural Graphene Quantum Dot/MnO2 Nanosheets toward High-Potential Window Electrodes for High-Performance Supercapacitors. *Advanced Science* **2018**, *5* (5), 1700887–1700887.
106) Huang, Y.; Lin, L.; Shi, T.; Cheng, S.; Zhong, Y.; Chen, C.; Tang, Z. Graphene quantum dots-induced morphological changes in CuCo2S4 nanocomposites for supercapacitor electrodes with enhanced performance. *Applied Surface Science* **2019**, *463*, 498–503.
107) Lv, H.; Yuan, Y.; Xu, Q.; Liu, H.; Wang, Y.-G.; Xia, Y. Carbon quantum dots anchoring MnO 2 /graphene aerogel exhibits excellent performance as electrode materials for supercapacitor. *Journal of Power Sources* **2018**, *398*, 167–174.
108) Chang, H.-W.; Fu, J.-X.; Huang, Y.-C.; Lu, Y.-R.; Kuo, C.-H.; Chen, J.-L.; Chen, C.-L.; Lee, J.-F.; Chen, J.-M.; Tsai, Y.-C.; Chou, W. C.; Dong, C.-L. NiCo2O4/graphene quantum dots (GQDs) for use in efficient electrochemical energy devices: An electrochemical and X-ray absorption spectroscopic investigation. *Catalysis Today* **2020**, *348*, 290–298.
109) Zhang, X.; Zhang, Y.; Wang, Y.; Kalytchuk, S.; Kershaw, S. V.; Wang, Y.; Wang, P.; Zhang, T.; Zhao, Y.; Zhang, H.; Cui, T.; Wang, Y.; Zhao, J.; Yu, W. W.; Rogach, A. L. Color-Switchable Electroluminescence of Carbon Dot Light-Emitting Diodes. *ACS Nano* **2013**, *7* (12), 11234–11241.
110) Kadian, S.; Sethi, S. K.; Manik, G. Recent advancements in synthesis and property control of graphene quantum dots for biomedical and optoelectronic applications. *Materials Chemistry Frontiers* **2021**, *5* (2), 627–658.
111) Choi, S. H. Unique properties of graphene quantum dots and their applications in photonic/electronic devices. *Journal of Physics D: Applied Physics* **2017**, *50* (10), 103002–103002.
112) Roy, P.; Periasamy, A. P.; Chuang, C.; Liou, Y.-R.; Chen, Y.-F.; Joly, J.; Liang, C.-T.; Chang, H.-T. Plant leaf-derived graphene quantum dots and applications for white LEDs. *New J. Chem.* **2014**, *38* (10), 4946–4951.
113) Chen, Y.-X.; Lu, D.; Wang, G.-G.; Huangfu, J.; Wu, Q.-B.; Wang, X.-F.; Liu, L.-F.; Ye, D.-M.; Yan, B.; Han, J. Highly Efficient Orange Emissive Graphene Quantum Dots Prepared by Acid-Free Method for White LEDs. *ACS Sustainable Chemistry & Engineering* **2020**, *8* (17), 6657–6666.
114) Tetsuka, H.; Nagoya, A.; Fukusumi, T.; Matsui, T. Molecularly Designed, Nitrogen-Functionalized Graphene Quantum Dots for Optoelectronic Devices. *Advanced Materials* **2016**, *28* (23), 4632–4638.
115) Gupta, V.; Chaudhary, N.; Srivastava, R.; Sharma, G. D.; Bhardwaj, R.; Chand, S. Luminscent Graphene Quantum Dots for Organic Photovoltaic Devices. *Journal of the American Chemical Society* **2011**, *133* (26), 9960–9963.
116) Kwon, W.; Kim, Y.-H.; Lee, C.-L.; Lee, M.; Choi, H. C.; Lee, T.-W.; Rhee, S.-W. Electroluminescence from Graphene Quantum Dots Prepared by Amidative Cutting of Tattered Graphite. *Nano Letters* **2014**, *14* (3), 1306–1311.
117) Kim, D. H.; Kim, T. W. Ultrahigh current efficiency of light-emitting devices based on octadecylamine-graphene quantum dots. *Nano Energy* **2017**, *32*, 441–447.
118) Kumar, M.; Kumar, A.; Sunny,; Seong, K.-S.; Park, S.-H. Single-Crystalline ZnO/Graphene Quantum Dots Phosphors-Converted White Light-Emitting Diodes. *IEEE Photonics Technology Letters* **2019**, *31* (3), 203–205.
119) Kumar, G. S.; Thupakula, U.; Sarkar, P. K.; Acharya, S. Easy extraction of water-soluble graphene quantum dots for light emitting diodes. *RSC Advances* **2015**, *5* (35), 27711–27716.
120) Kim, H. J.; Lee, C. K.; Seo, J. G.; Hong, S. J.; Song, G.; Lee, J.; Ahn, C.; Lee, D. J.; Song, S. H. Highly luminescent polyethylene glycol-passivated graphene quantum dots for light emitting diodes. *RSC Advances* **2020**, *10* (46), 27418–27423.
121) J, K. K.; Bae, S.; Yi, Y.; Jin Park, M.; Jin Kim, S.; Myoung, N.; Lee, C.; Hee Hong, B.; ; Hyeok Park, J. Origin of white electroluminescence in graphene quantum dots embedded host/guest polymer light emitting diodes. *Origin of white electroluminescence in graphene quantum dots embedded host/guest polymer light emitting diodes. Scientific reports* **2015**, *5*, 1–11.
122) Kwon, W.; Kim, Y.-H.; Kim, J.-H.; Lee, T.; Do, S.; Park, Y.; Jeong, M. S.; Lee, T.-W.; Rhee, S.-W. High Color-Purity Green, Orange, and Red Light-Emitting Diodes Based on Chemically Functionalized Graphene Quantum Dots. *Scientific Reports* **2016**, *6* (1), 1–10.
123) Lin, T.-N.; Santiago, S. R. M.; Yuan, C.-T.; Chiu, K.-P.; Shen, J.-L.; Wang, T.-C.; Kuo, H.-C.; Chiu, C.-H.; Yao, Y.-C.; Lee, Y.-J. Enhanced Performance of GaN-based Ultraviolet Light Emitting Diodes by Photon Recycling Using Graphene Quantum Dots. *Scientific Reports* **2017**, *7* (1), 1–9.
124) Luk, C. M.; Tang, L. B.; Zhang, W. F.; Yu, S. F.; Teng, K. S.; Lau, S. P. An efficient and stable fluorescent graphene quantum dot–agar composite as a converting material in white light emitting diodes. *Journal of Materials Chemistry* **2012**, *22* (42), 22378–22378.

125) Li, W.; Li, M.; Liu, Y.; Pan, D.; Li, Z.; Wang, L.; Wu, M. Three Minute Ultrarapid Microwave-Assisted Synthesis of Bright Fluorescent Graphene Quantum Dots for Live Cell Staining and White LEDs. *ACS Applied Nano Materials* **2018**, *1* (4), 1623–1630.